Volume 62
Number 21
17 March 2026
Pages 5769–5992

ChemComm

Chemical Communications

rsc.li/chemcomm

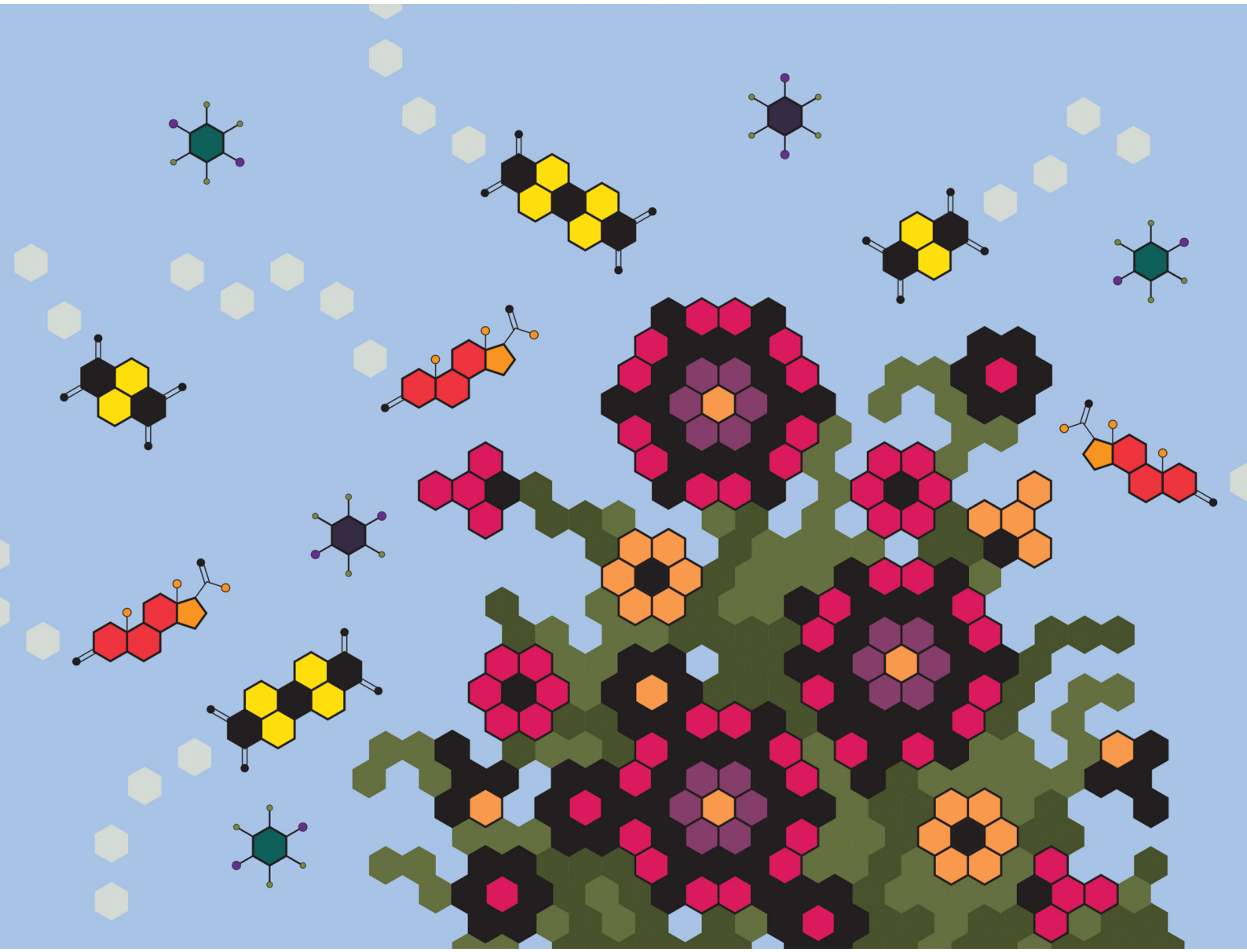

ISSN 1359-7345

ROYAL SOCIETY OF CHEMISTRY

FEATURE ARTICLE
Jogirdas Vainauskas and Tomislav Friščić
Cocrystallisation with carbon

ChemComm

FEATURE ARTICLE

View Article Online
View Journal | View Issue

Cite this: *Chem. Commun.*, 2026, **62**, 5780

Cocrystallisation with carbon

Jogirdas Vainauskas *[ab] and Tomislav Friščić *[ab]

Received 12th November 2025,
Accepted 8th January 2026

DOI: 10.1039/d5cc06433c

rsc.li/chemcomm

While carbon is ubiquitous across organic synthesis and materials chemistry, in supramolecular chemistry the role of carbon as a target for the formation of directional interactions, such as hydrogen or halogen bonds, is less known and developed in comparison to nitrogen or oxygen. Here we provide a brief review of the opportunities for the design of multi-component crystals (cocrystals) based on the recognition of carbon-based moieties, notably non-substituted polycyclic aromatic hydrocarbons (PAHs), functionalities bearing single carbon atom recognition sites such as isonitriles or carbenes, as well as the molecules of the element carbon itself, such as fullerenes, with particular emphasis on halogen bonding and C–H···π interactions. By providing highlights of historical examples, as well as select recent advances including applications oriented towards carbon nanomaterials, this review illustrates the role of carbon in cocrystallisation and solid-state supramolecular chemistry, from fundamental research and materials design, to biomolecular recognition and extraterrestrial geology.

Introduction

Carbon is the central element of organic chemistry, and the basis of organic materials science. In the context of supramolecular chemistry, however, the value of carbon as a target of molecular recognition and design of supramolecular architectures is easily overshadowed by the neighboring elements of the periodic table, such as nitrogen or oxygen. Understanding and controlling the supramolecular chemistry of carbon-based moieties, however, is known to be of considerable significance in areas such as biochemistry[1] and materials chemistry. In the latter context, and focusing on organic solids, aromatic carbon-based moieties are ubiquitous in functional organic materials, providing stability, access to well-established

[a] *School of Chemistry, University of Birmingham, Edgbaston, Birmingham B152TT, UK. E-mail: t.friscic@bham.ac.uk, jxv258@student.bham.ac.uk*
[b] *Department of Chemistry, McGill University, 801 Sherbrooke St. W., H3A0B*, Montreal, Canada. E-mail: tomislav.friscic@mcgill.ca, jogirdas.vainauskas@mail.mcgill.ca*

Jogirdas Vainauskas

Jogirdas Vainauskas received his B.Sc. in Chemistry (2020) from McGill University, where he subsequently continued his PhD studies under the supervision of Prof. Tomislav Friščić. Following time abroad at the University of Birmingham, he received his PhD in Chemistry (2025) from McGill University. His research examines experimental and theoretical aspects of solid-state supramolecular chemistry, focusing on materials with new optical/electronic properties, as well as cocrystal design using supramolecular recognition of carbon-based units.

Tomislav Friščić

Tomislav Friščić is a Leverhulme International Chair at the University of Birmingham. He received a B.Sc. in Chemistry with Branko Kaitner (University of Zagreb), PhD with Leonard MacGillivray (University of Iowa), followed by post-doctoral research with William Jones, Pfizer Institute for Pharmaceutical Materials Science, and Herchel Smith Fellowship (University of Cambridge). He is a Fellow of the Royal Society of Chemistry and corresponding member of Croatian Academy of Sciences and Arts. His group's work spans mechanochemistry, crystal engineering, materials and green chemistry, with awards including ACS National Award for Affordable Green Chemistry, RSC Corday-Morgan Medal, NSERC John C. Polany Award.

synthetic approaches that can address multiple functionalisation sites, and can exhibit tunable electronic properties. The solid-state crystalline environment of such aromatic moieties affects diverse materials properties, such as reactivity,[2–4] conductivity,[5,6] or luminescence.[7] A pertinent example is the organic semiconductor pentacene, where the solid-state molecular arrangement (*i.e.*, the crystal "packing") has a profound effect on the electronic properties of the crystalline solid.[8] Whereas pristine pentacene crystallises with molecules adopting a herringbone arrangement, the covalent attachment of steering groups onto the pentacene core can promote face-to-face molecular stacking, enhancing conductivity *via* increased π-orbital overlap.[9]

The sensitivity of the crystal packing to molecular structure[10] means that the crystalline arrangement of aromatic carbon-based moieties can, in principle, be readily altered through covalent derivatisation. Such a strategy is exemplified by introducing halogen substitution to encourage β-stacking of cinnamic acid derivatives to achieve predictable, solid-state photochemical reactivity.[4] Covalent derivatisation, however, inherently modifies the electronic properties, and potentially also the shape, of target molecules, which could impact the sought properties in an undesired way. The design of cocrystals,[11] *i.e.* a class of materials containing two or more molecular components in the same crystalline structure, is an alternative strategy to modify solid-state properties, focusing on intermolecular interactions to guide molecular self-assembly. Cocrystallisation permits aromatic carbon-based moieties to be rearranged within a crystal structure and carefully positioned to promote a certain type of functional behavior,[12] modify or generate properties, without requiring more heavy-handed chemical derivatisation approaches.[13] Cocrystal design has historically often relied on the presence of functional groups that can engage in directional intermolecular interactions, such as hydrogen (HB) or halogen bonding (XB), often targeting electron-rich heteroatoms such as N, O, S, as recognition sites.[14,15] Certain functional groups are particularly adept at forming homo- or hetero-molecular interactions of robust geometry, enabling their use as supramolecular building units, or supramolecular synthons,[16] for cocrystal design. In the context of hydrogen bonding, this includes homosynthons such as carboxylic acid-acid dimers, amide ladders, and hydroxyl chains, as well as heterosynthons such as carboxylic acid-amide dimers, hydroxyl-pyridine HBs, carboxylic acid-pyridine HBs.[17] Supramolecular synthons are typically described using a graph-set approach, recently expanded to include other types of interactions, such as halogen bonds.[18] Nevertheless, while there are also non-directional supramolecular motifs involving carbon-only based moieties, such as different types of π-stacking, supramolecular synthons based on directional interactions to carbon are considered unconventional and not traditionally considered in cocrystal design.

This article highlights the role of carbon in molecular recognition and cocrystal formation, illustrating how the use of interactions different from traditional, non-directional π-stacking, gives rise to a rich, rapidly-expanding landscape of carbon-based cocrystal materials, with relevance from biomolecular recognition and materials design to molecular assembly in extraterrestrial environments. We perceive strategies for supramolecular recognition and manipulation of non-substituted, carbon-only molecular skeletons, such as those of polycyclic aromatic hydrocarbons (PAHs) and fullerenes, to be highly important for advancing the development of materials such as graphenes, carbon nanotubes (CNTs), and covalent-organic frameworks (COFs).[19,20] Indeed, supramolecular recognition of such carbon-based species using directional, site-specific interactions, without any covalent modification, can be seen as a stimulating challenge of crystal engineering. In our view, cocrystallisation of carbon-rich and hydrocarbon moieties using such interactions could be seen as a supramolecular equivalent of C–H activation[21] – a topic that has over the past decades led to exciting developments in the covalent chemistry of carbon. This review is written with the intention to inspire similar excitement in the area of solid-state chemistry and materials design, by highlighting the rich but too-often overlooked potential of carbon as an element of crystal engineering.

Assembly through π-stacking

It is impossible to discuss the recognition of carbon-only molecular moieties without addressing the non-directional π-stacking of aromatic units, widely present across supramolecular chemistry and biology, and known to be crucial for the structural stability of various carbon-based materials, including COFs,[22,23] nucleic acids,[24] or proteins.[25] A full overview of π-stacking in biochemistry, supramolecular chemistry and crystal engineering is certainly beyond the scope of this work,but further information can be found in available reviews.[1,26–30] While the exact nature of such interactions remains an active area of research,[31,32] the stacking motifs discussed here will broadly encompass any interaction that can lead to recognition and parallel alignment of molecules along the carbon-based aromatic systems. While keeping in mind that the use and precise definitions of the terms π···π interactions and π-stacking are sometimes a source of discussion,[33] these terms have in general proven to be highly effective as geometric descriptors in structural analysis of molecular solids, and are vital to the current understanding of crystal engineering.

Although π···π stacking between π-systems of similar quadrupole moments,[34] is commonly found in single- and multi-component solids, there appears to be limited scope to design cocrystals *via* such interactions. This is evident from the observation that there are very few structural reports of cocrystals based on π···π stacking of different PAHs,[35] yet such stacking is frequently seen as crucial in crystal structures of pristine PAHs.[36]

The use of π···π stacking for cocrystal design can rely on combining it with other, stronger intermolecular interactions. This means relying on π···π stacking as a secondary interaction for structure "fine-tuning".[37,38] For example, O–H···N hydrogen bonding to pyridine-like bases was used as a primary supramolecular synthon, while pyridine units further associate

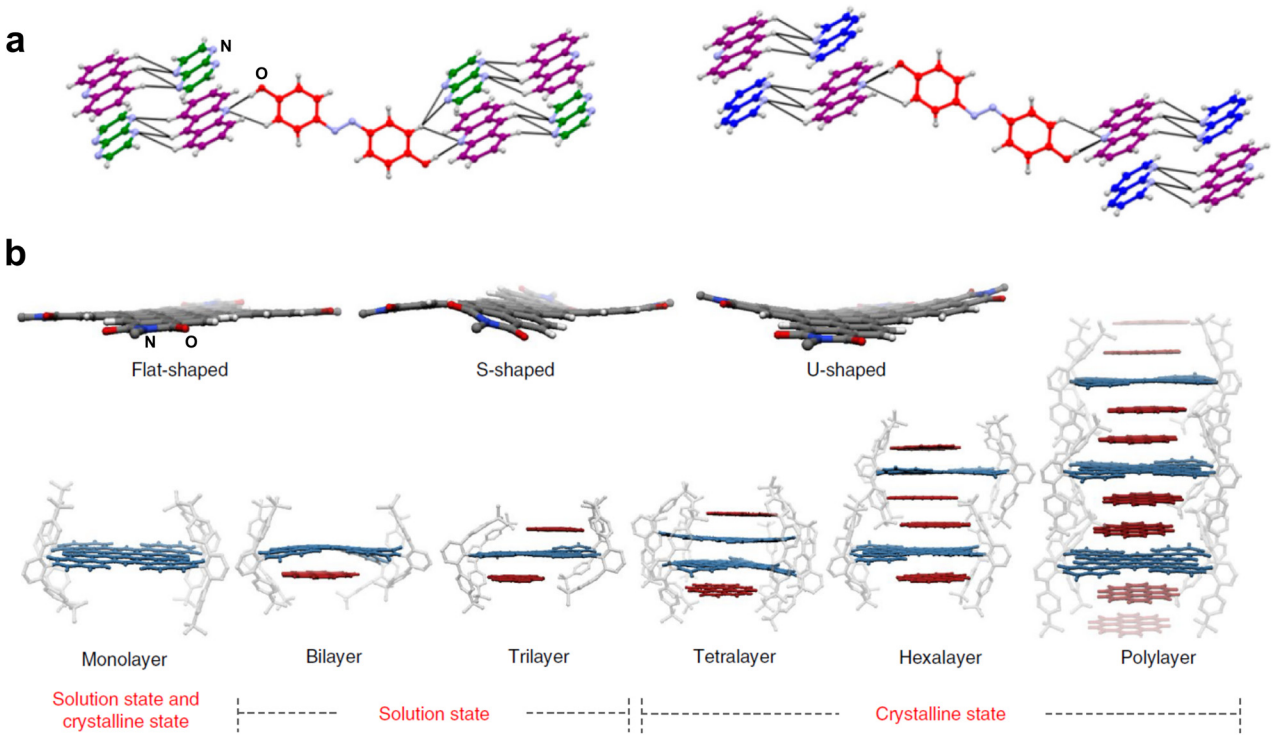

Fig. 1 (a) Cocrystals assembled through the combination of O–H···N HBs and π···π stacking (adapted with permission.[39] Copyright 2014, American Chemical Society). (b) Nanographene-based cocrystals with coronene assembled through π···π stacking (adapted with permission[41] from SNCSC).

through π···π stacking to generate binary and ternary cocrystals (Fig. 1a).[39]

Theoretical calculations indicate that interactions between π-systems become stronger with increasingly large aromatic surfaces, as a result of greater dispersion contributions.[40] Consequently, cocrystal design based primarily on π···π stacking has been most successful when applied to molecules with extended aromatic systems, such as nanographenes and larger PAHs. As an example, the Würthner group has reported several nanographene systems which form cocrystals with PAHs, arranging into a variety of stacking assemblies.[41–43] In one example,[41] a C_{64} nanographene unit was found to form complexes of different compositions with PAHs, yielding stoichiometrically different cocrystals (stoichiomorphs). Using coronene (**cor**) as a cocrystal former (coformer) led to cocrystals comprising discrete **cor**···C_{64}···C_{64}···**cor** tetramers, **cor**···C_{64}···**cor**···**cor**···C_{64}···**cor** hexamers, or infinite **cor**···C_{64}···**cor** columnar stacks (Fig. 1b), with typical **cor**···C_{64} distances in the 3.2–3.4 Å range. The large accessible π-surface of the nanographene is well-suited for π···π stacking, while any sterically demanding groups on the periphery of the molecule inhibit rapid self-complexation, thereby promoting stacking-based cocrystallisation and isolation of PAH dimers within the stacked structure. Niyas *et al.*[42] demonstrated the ability of a flexible nanographene to form ternary cocrystals based on π···π stacking and allosteric regulation: upon initial complexation with a phthalocyanine-based coformer, the nanographene was found to undergo a distortion which inhibited secondary phthalocyanine binding on the opposite side of the nanographene unit, but still could accommodate complexation with a smaller PAH. In this way, ternary cocrystals can be formed as a result of active deformation of π-surfaces, offering a shape-based pathway for selective cocrystallisation.

Polar···π stacking

Stacking interactions between electron-rich and -deficient aromatic systems are a widely studied and applied type of carbon-based recognition motifs in cocrystal design. Such polar···π stacking, or the formation of donor–acceptor complexes, is not only a highly reliable motif, but can also engage an immense variety of molecules or functionalities.[44] Examples of electron-deficient coformers include perfluoroarenes, cyano- and nitro-decorated molecules (tetracyanobenzene, tetracyanoquinodimethane, nitrobenzenes), aromatic anhydrides, diimides, and more, providing the crystal engineer a large pool of molecules to ponder and choose from in cocrystal design. Additionally, many molecules are readily functionalised to incorporate electron-rich or -deficient moieties, which facilitates the installation of groups capable of polar···π interactions as a cocrystal design strategy.

Arene···perfluoroarene stacking is highly popular in cocrystal design, originating from the early study of the now archetypal cocrystal (benzene)(hexafluorobenzene).[45] Cocrystals containing hexafluorobenzene most commonly contain nearly co-facial A–B–A–B stacking motifs involving aromatic stacking partners such as *p*-xylene,[46] mesitylene,[47] or *N*,*N*-dimethylaniline.[48] The reliability of arene···perfluoroarene stacking, which has cemented the use of such interactions in cocrystal design, is demonstrated by the tolerance of the resulting self-assembly motifs to molecular size. For example, Collings *et al.*[49] have

demonstrated the reliable formation of 1 : 1 stoichiometry cocrystals of octafluoronaphthalene with a number of differently-sized PAHs, including anthracene, phenanthrene, pyrene, or triphenylene. In all cases, the cocrystal structures comprised alternating arene···perfluoroarene stacks interconnected *via* C–H···F hydrogen bonds. Analysis of hexafluorobenzene cocrystals with several PAHs suggests that the two cocrystal components will be positioned in a way to minimise electrostatic repulsion between the electron-rich fluorine atoms and the electron-rich PAH surface, offer a way to anticipate the final molecular orientations in the cocrystal.[50]

The reliability of phenyl···perfluorophenyl stacking was used in the design of functional, reactive cocrystals, as shown by the Grubbs group who exploited such interactions to align butadiyne moieties in the solid state, facilitating topochemical polymerisation into then unprecedented *cis*-polydiacetylenes.[51] The same strategy was expanded to [2+2] photo-dimerisation and -polymerisation in cocrystals containing mono- and diolefins (Fig. 2a), with near-quantitative photoproduct yields in some cases.[52] The Frauenrath group has explored phenyl···perfluorophenyl stacking in combination with flexible ester-containing butadiynes,[53] yielding cocrystals that undergo topochemical polymerisation to selectively form alternating phenyl–perfluorophenyl poly(diacetylene) molecules (Fig. 2b). The phenyl···perfluorophenyl stacking is retained upon introducing alkyl chains onto phenyl ring-derivatives, yielding highly-soluble poly(diacetylenes).[54] Other photoreactive cocrystals based on phenyl···perfluorophenyl stacking have explored diphenylhexatrienes,[55] triacetylenes,[56] as well as a non-symmetrical olefin as a reactant towards the formation of a tetra-substituted cyclobutane (Fig. 2c).[57] Although not based on a cocrystal, the solid-state photochemical synthesis of a COF directed by phenyl···perfluorophenyl stacking by the King group is notable as a feat of crystal engineering-based materials synthesis.[58]

The stacking geometries are well-suited for promoting pressure-induced reactivity in organic solids,[59] allowing aromatic rings to be compressed within a reactive distance of 2.6 Å.[59,60] Pressure-induced chemical reactivity has been reported for alternating-stack cocrystals composed of arenes and perfluoroarenes, yielding extended sp^3-hybridised carbon species. With increasing pressure, the (benzene)(hexafluorobenzene) cocrystal was found to undergo several polymorphic transitions and a [4+2] Diels–Alder reaction to generate columnar hydrofluorocarbons,[61] with further increases in pressure leading to a fluorinated graphane structure.[62] Similarly, columnar hydrofluorocarbons were found to be generated by exposing cocrystals such as (octafluoronaphthalene)(naphthalene) and (octafluoronaphthalene)-(anthracene) to pressures of *ca.* 20–25 GPa.[63,64]

While the formation of arene···perfluoroarene stacking motifs is generally predictable, anticipating intermolecular interactions perpendicular to the stacking axis is often more difficult. An in-depth report by Colombo *et al.*[35] combined theoretical calculations and analysis of the Cambridge Structural Database (CSD) to investigate packing motifs in binary 1 : 1 cocrystals involving polar···π stacking; examining a broad subset of molecular components, the cocrystal structures

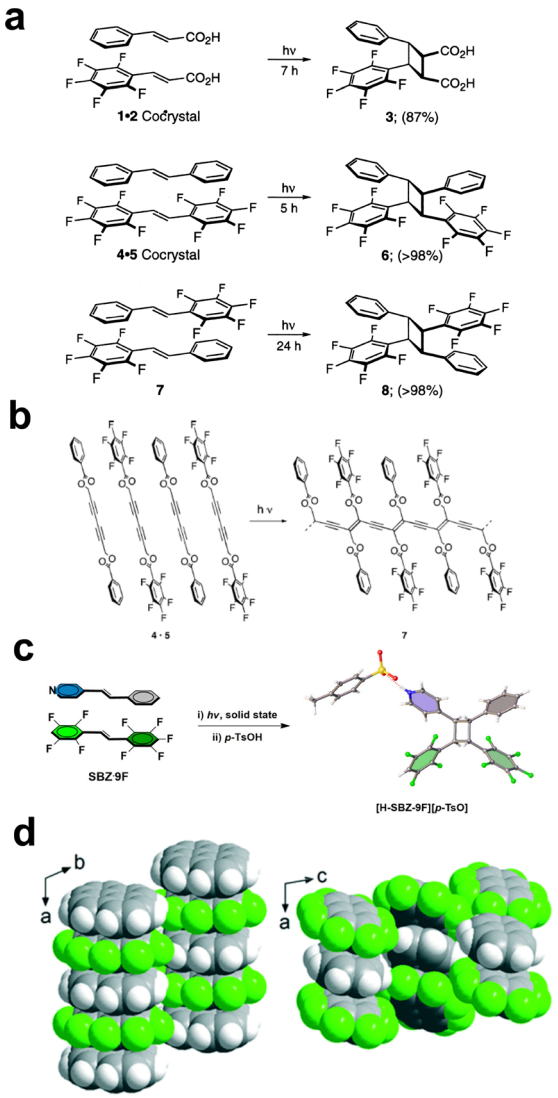

Fig. 2 (a) Topochemical [2+2] photocycloaddition templated in cocrystals by phenyl···perfluorophenyl stacking (adapted with permission.[52] Copyright 1998, American Chemical Society). (b) Topochemical polymerisation templated in cocrystals by phenyl···perfluorophenyl stacking (adapted with permission.[53] Copyright 2006, American Chemical Society). (c) Solid-state synthesis of a four-substituent cyclobutane *via* a phenyl···perfluorophenyl stacking cocrystal (adapted with permission[57] from SNCSC). (d) Alternate ladder (left) and slanted-column (right) stacking motifs in polar···π cocrystals (adapted from ref. 35).

were found to commonly contain infinite A···B···A···B stacked columns, with A···B interaction energies in the range 25–60 kJ mol^{-1}. The packing of such stacked units, however, varied widely (Fig. 2d), and depended both on the choice of stacking partners and the presence of secondary weaker interactions, such as C–H···N hydrogen bonding.

Combining weak interactions with molecular shape-fitting can offer greater control over packing of stacking assemblies, as illustrated by a recent study by Alfuth *et al.*[65] A series of cocrystals involving perfluorophenol and triaryl coformers showed that the perfluorophenol units form hydrogen-bonded

trimers which stack with triaryl coformers through phenyl···perfluorophenyl interactions. In directions perpendicular to the stacking axis, the perfluorophenol trimers sit in pockets lined with C–H···F interactions, yielding layers of two-dimensional (2D) triangle-based tilings (Fig. 3a). The importance of shape matching is especially relevant considering that C–H···F interactions are not seen as strongly structure directing.[66,67]

While the polar···π stacking interactions generally depend on electrostatic and dispersion contributions to bring electron-rich and -poor aromatic systems into close contact, certain electron-poor coformers additionally lead to considerable charge-transfer behaviour upon stacking. Tetracyanobenzene and tetracyanoquinodimethane are two such coformers, well-established in the design of charge-transfer cocrystals, yielding materials with unique optical and luminescence properties.[68–72] Trinitrobenzene has also been extensively studied as a component in charge-transfer cocrystals,[73–75] assembling into polar···π stacking structures with a wide range of aromatic coformers. The Desiraju group explored a variety of such trinitrobenzene-based systems,[76,77] examining the role of C–H···O hydrogen bonds[78] for controlling the alignment of stacking structures. For example, this type of structural control was employed in the (1,3,5-trinitrobenzene)(triphenylene) cocrystal (Fig. 3b), demonstrating enhanced non-linear optical properties compared to the starting components.[79] Aromatic diimides are a particularly exciting class of coformers, possessing electron-poor core regions that are well-suited for cocrystal formation with electron-rich arenes.[80–86] Due to the vast number of different imide and core substituted diimides that have been synthesised, as well as arene coformers of different shapes and sizes, structural trends found in diimide cocrystals, apart from the presence of polar···π stacking, are highly diverse. For example, Gao *et al.*[80] examined a series of perylene diimide (**PDI**) cocrystals in which different aromatic coformers produced various structural motifs, composed of stacked heteromolecular trimers (arene···**PDI**···arene), dimers (arene···**PDI**) or an alternating stacking motif (Fig. 3c). The variability of stacking motifs is particularly evident in case of diimide macrocycles: the Stoddart group examined the packing motifs in cocrystals of triangular **NDI** macrocycles,[87,88] where the rigid three-dimensional (3D) shape and porosity of the macrocycle lead to different supramolecular "tessellations" (Fig. 3d), highly dependent on the choice of the aromatic coformer[89] and solvent of crystallisation.[81,90]

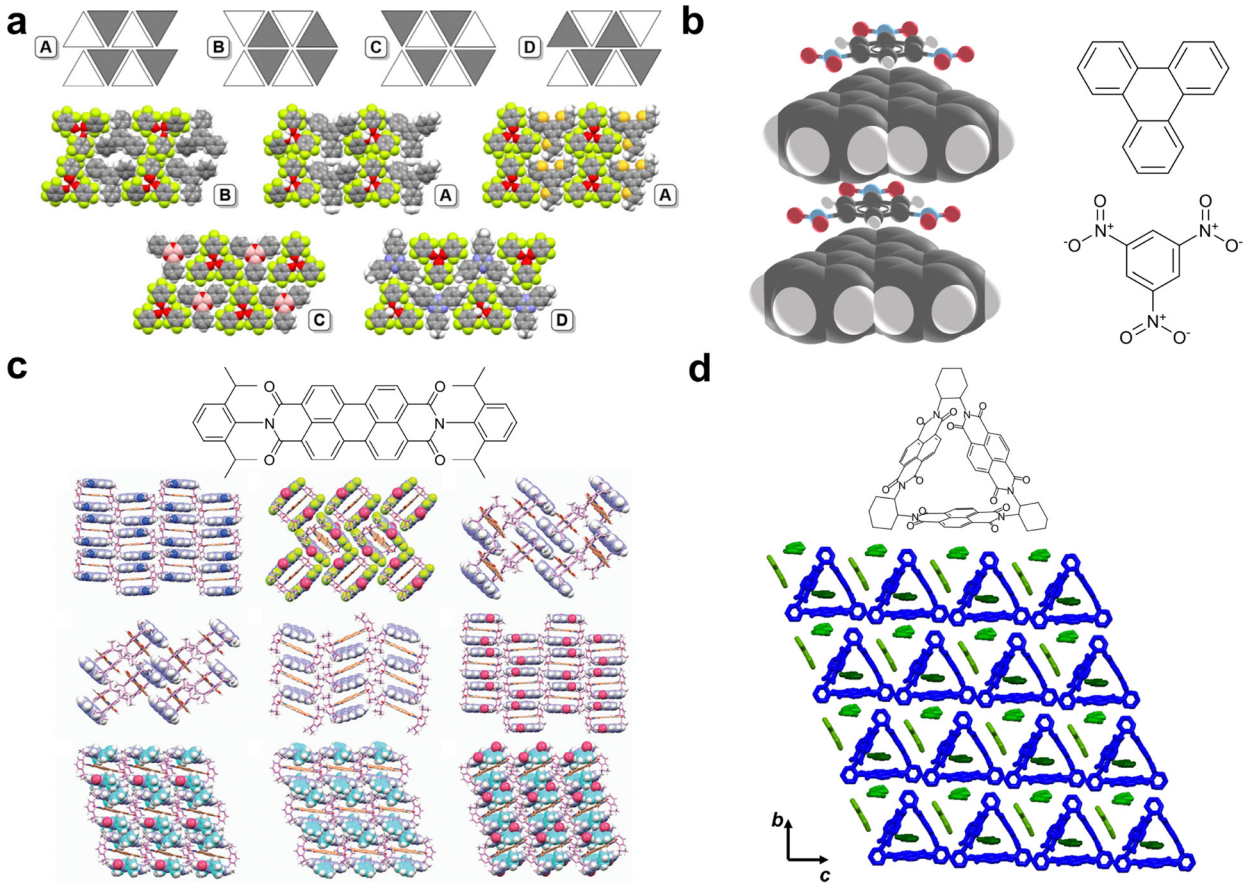

Fig. 3 (a) Triangular molecular tiling in cocrystals assembled through polar-π stacking and C–H···F interactions (adapted from ref. 65 under the terms of the CC-BY license). (b) Stacking structure in the (1,3,5-trinitrobenzene)(triphenylene) cocrystal.[79] (c) Packing motifs in **PDI** cocrystals with different aromatic coformers (adapted with permission.[80] Copyright 2024, Wiley). (d) Supramolecular tessellation in a NDI macrocycle cocrystal (adapted with permission.[81] Copyright 2019, American Chemical Society).

Halogen bonding

Early studies

Early investigations into solution systems containing dihalogens and PAHs revealed the appearance of charge-transfer between the two species,[91] with the charge-transfer complex of I_2 and benzene (C_6H_6) notably serving as a model system for Mulliken's studies of charge transfer phenomena.[92] Although Mulliken initially believed the complex consisted of I_2 molecules aligned in parallel on top of the arene π-system, other structural arrangements were also considered, including one with the I_2 molecule positioned perpendicular to the benzene plane. The latter model was eventually supported by the 1958 crystallographic analysis of (benzene)(Br_2) by Hassel and Strømme around 230 K.[93] The structure, which represents one of the earliest structural studies on a halogen-bonded cocrystal, is comprised of one-dimensional (1D) chains of alternating molecules of C_6H_6 and Br_2. The long axis of each Br_2 molecule was found to be normal to the aromatic plane of neighboring benzene molecules, indicating that directional Br–Br···π halogen bonding is responsible for the formation of the observed 1D chain structure. The structure was subsequently revisited by the Kochi group, who established that at 123 K the Br_2 molecule makes a particularly close contact to a pair of carbon atoms at the rim of the aromatic system (Fig. 4a) in (benzene)(Br_2), as well as in the analogous (toluene)(Br_2) cocrystal.[94] Both cocrystals were found to spontaneously generate HBr and yield either bromobenzene, or a mixture of *o*- and *p*-bromotoluene, upon sitting at 78 °C, indicating a direct connection between site-specific halogen bonding in the cocrystal and ring bromination.

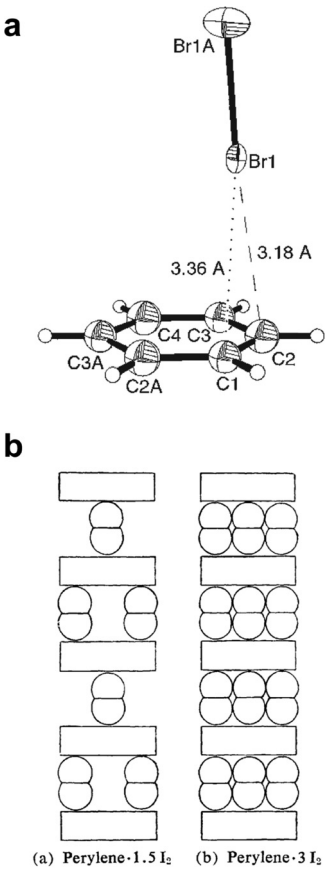

Fig. 4 (a) A halogen-bonded fragment from the (benzene)(bromine) cocrystal (adapted from ref. 94*a*). (b) Proposed structures for cocrystals of perylene and I_2 (adapted from ref. 101, by permission of the Bulletin of the Chemical Society of Japan).

The original report of the (benzene)(Br_2) structure was followed by analyses of a number of analogous cocrystals, including (C_6H_6)(Cl_2),[95] as well as cocrystals of Br_2 or I_2 with other aromatic hydrocarbons, including toluene and coronene[94] (CSD codes DUPCIA01, DUPCIA10). In all cases, a roughly perpendicular arrangement of the dihalogen molecule with respect to the arene plane was observed. Such arrangements are in general agreement with the more recent theoretical studies on the geometry of halogen bonding involving dihalogens with benzene or PAHs.[96–99] For example, theoretical studies by the groups of Hobza and of Kim groups[99] found that a halogen bond should form to the rim of a benzene molecule, while a combined theoretical and database study by Ang *et al.*[97] indicated similar preferences for benzene, as well as larger PAHs. It is, however, possible that halogen bonding preferences of dihalogens towards PAHs change with increasing size of the aromatic system, as indicated by modelling studies by Kim *et al.* on flat PAHs, and by Cabaleiro-Lago and Rodríguez-Otero on curved systems. These studies found that dihalogens interacting with large polycylic aromatic sheets might preferably engage in side-on interactions, rather than halogen bonding.[98]

The formation of halogen-bonded cocrystals of dihalogens and PAHs can also lead to materials with interesting electrical properties, as illustrated by conductive behavior that was noted for systems containing pyrene or perylene with Br_2 or I_2.[100,101] Akamatu *et al.*[100] reported that the addition of Br_2 to a solution of perylene in C_6H_6 produces a black precipitate, comprising three or four Br_2 molecules per each perylene unit. Freshly prepared samples were found to exhibit low resistivity (tens of Ω cm^{-1}), stated at the time to be the smallest for a simple organic compound excepting graphite and carbons.[100] Although crystal structures do not appear to have been reported for these solid-state complexes, models based on spacing of crystallographic planes obtained from powder X-ray diffraction (PXRD) data indicate structures are again based on XBs to π-systems (Fig. 4b).[101]

Halogen-bonded supramolecular synthons for PAH cocrystallisation

Cocrystals based on XBs to π-systems have for a long time been limited to the outlined dihalogen–PAH complexes, with sparing examples involving other small XB donors, such as tetrabromomethane (CBr_4).[102,103] Research over the past two decades, however, strongly points to XBs to carbon-based π-systems as reliable directional interactions that can be accessed through a variety of halogen bond donors, enabling the design and synthesis of a wide range of cocrystals exhibiting robust, reliable supramolecular motifs. Whereas this overview is focusing on crystal engineering and self-assembly in the solid state,

it is notable that halogen bonding to carbon-based π-systems has also been studied in gas phase and solution environments.[104] The possibility of PAHs to engage in halogen bonding was explored by the Jin group, who reported a number of halogen-bonded cocrystals with small-molecule arenes or heterocycles, including carbazole,[105] fluorene and its derivatives,[106] acenaphthene,[107] biphenyl, and others.[108–112] Notably, Shen *et al.*[112] reported cocrystals of 1,4-diiodotetrafluorobenzene (**14tfib**) XB donor with naphthalene or phenanthrene as acceptors, exhibiting ladder-like motifs arranged through C–I···π interactions. In each cocrystal, the PAH units that act as rungs of the ladder engage in four XBs to the **tfib** donor molecules acting as rails. The shortest C–I···π contacts form either to the center of a carbon–carbon bond in the arene, or directly to a carbon atom, with C–I···C distances between 3.43–3.63 Å, which is *ca.* 1–7% shorter from the expected sum of the van der Waals radii of iodine and carbon.[113]

Such ladder-like self-assembly motifs, involving **14tfib** and unsubstituted aromatic systems, were subsequently found to tolerate significant variations in the size and shape of the PAH acceptor,[114] as demonstrated by a systematic array study with acceptors ranging from the single-ring benzene molecule to the 15-ring dicoronylene unit. The C–I···π ladder motif was found in case of eight out of nine explored PAHs which, in terms of the supramolecular yield concept introduced by Aakeröy and coworkers,[115] represents an interaction with a high supramolecular yield of 89%. Comparison of the experimentally determined crystal structures to electrostatic surface potential (ESP) calculations revealed that, in most cases, the C–I···π halogen bonds formed towards regions of the PAH exhibiting the largest negative ESP, indicating potential for recognition site selectivity[97] even with halogen bond donors more complex than dihalogens. The halogen bond interaction energies, based on periodic density-functional theory (DFT) calculations, were found to span *ca.* 13–21 kJ mol^{-1}, in general agreement with other theoretical studies on C–I···π halogen bonds.[116,117] Overall, the C–I···π ladder motif, and related architectures, have been observed across a wide number of PAH cocrystals (Fig. 5), indicating a robust supramolecular synthon applicable to engineering cocrystals using directional interactions to non-substituted hydrocarbons.

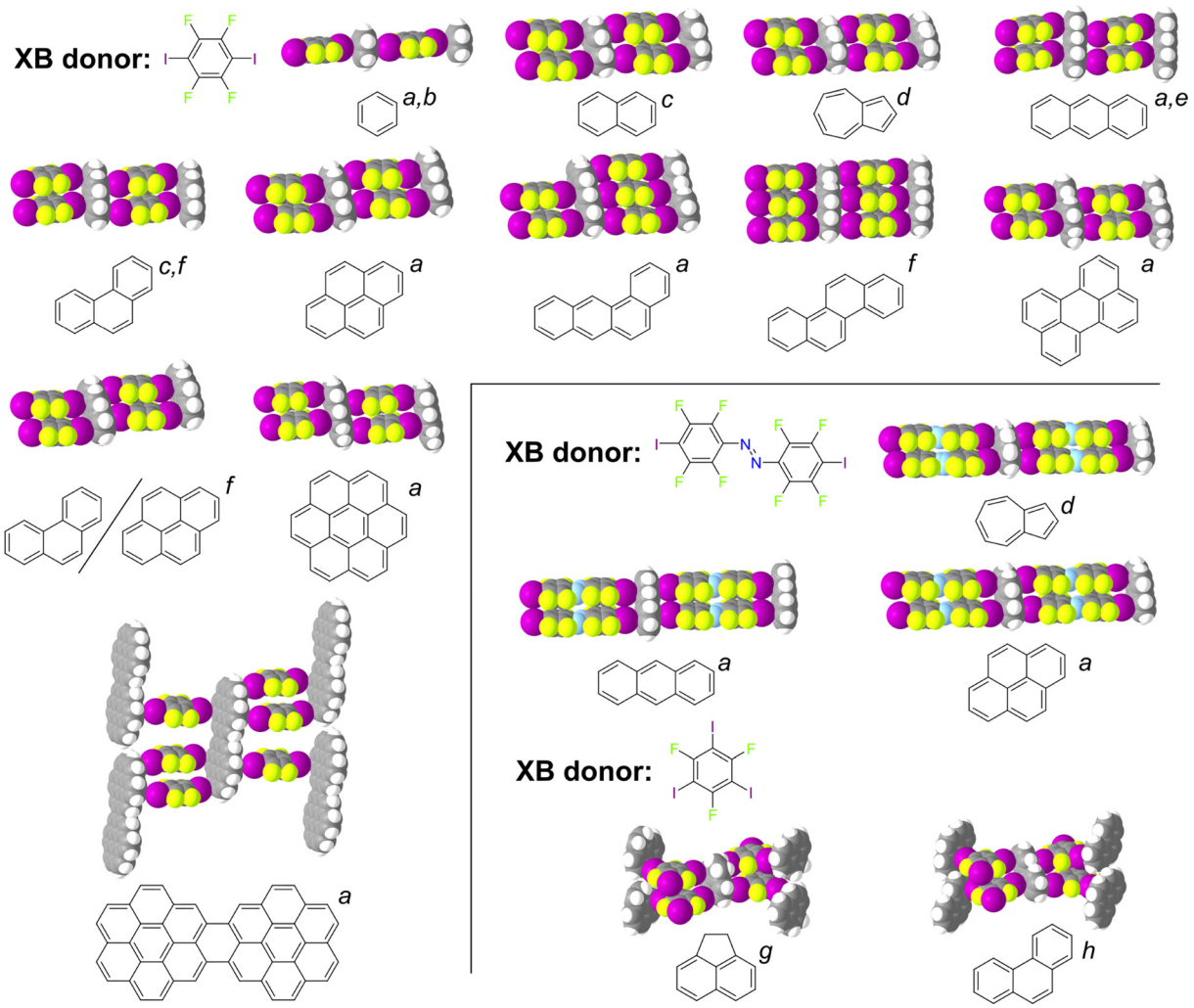

Fig. 5 Selected examples of cocrystal structures of differently-sized and -shaped PAHs and related molecules with **tfib** and other XB donors, illustrating the frequent appearance of C-I···π ladder motifs. References: a,[114] b,[119] c,[112] d,[127] e,[128] f,[129] g,[107] and h.[111]

Robustness of halogen bonding to carbon π-systems

Analyses of the CSD[97,114] support the view of C–I···π halogen bonding as a robust interaction, with a tendency for directional behavior across a wide range of geometrically- and electronically-distinct carbon-based acceptors, including unsaturated five-, six- or seven-membered rings, C=C double bonds, as well as C≡C triple bonds. The robustness of the interaction is illustrated by the structures of the three stoichiomorphs of the cocrystal of **14tfib** and pyrene:[109,114,118] whereas only the (**pyrene**)(**14tfib**)$_2$ cocrystal[114] exhibits the supramolecular ladder motif, its stoichiometric variations (**pyrene**)(**14tfib**) and (**pyrene**)$_4$(**14tfib**) all contain short I···π halogen bonds. A systematic study of *p*-xylene cocrystallisation with fluorobenzene derivatives demonstrated a similar tendency for the formation of halogen bonds to π-systems when using bromine- or iodine-substituted coformers.[119] Whereas different XB donors, such as 1,3,5-triiodo-2,4,6-trifluorobenzene (**135tftib**), have been used to form C–I···π halogen-bonded cocrystals with arenes, resulting structural motifs were found to vary depending on the choice of XB donor.[107,111] Comparing the cocrystallisation behavior of bromine- and iodine-substituted XB donors led the Jin group to propose the difference in ESPs as a guideline for determining whether cocrystallisation will result in XBs to π-systems or in π···π stacking interactions.[111]

Stepping away from fluorinated halogen-bond cocrystal formers, the Bosch group reported cocrystals of 1,4-diiodotetrachlorobenzene (**14tcib**) as the donor, with either benzene or naphthalene as the acceptor, comprising halogen-bonded chain motifs assembled through I···π halogen bonds.[120] Varying structural motifs are also observed when targeting non-PAH XB acceptors.[121,122] For example, d'Agostino *et al.*[123] reported stoichiomorphic cocrystals of **14tfib** with tolane and *trans*-stilbene, based on XBs to phenyl moieties. The cocrystal consisting of the XB donor and the arene in a 1 : 1 stoichiometric ratio adopted a structure with each phenyl ring engaged in a single XB, whereas a 2 : 1 stoichiometric ratio led again to a sheet structure reminescent of the C–I···π ladder, with two XBs to each of the hydrocarbon phenyl rings (Fig. 6a). Changes to composition and crystal structure also led to differences in luminescent behavior, with the cocrystal of 1 : 1 stoichiometric composition exhibiting fluorescence, and the 1 : 2 cocrystal being phosphorescent.[123]

Although extended π-systems provide ample recognition points for C–X···π halogen bonding (X = Br, I), commonly used XB donors with electron-deficient aromatic cores can also simultaneously interact with such π-systems through polar-π stacking interactions. Jain *et al.*[118] outlined multiple approaches to designing halogen-bonded three-component (ternary) cocrystals, including the tandem use of stacking interactions and C–I···π XBs. This led to several ternary cocrystals where **14tfib** was found to engage in stacking interactions and XBs with pyrene, while pyrene units also subsequently stack with a third component (Fig. 6b). This design approach was successful for forming ternary cocrystals containing **14tfib** and pyrene along with 4-nitrobenzaldehyde, 1,4-dinitrobenzene, 1,4-dicyanobenzene, or 1,4-diiodobenzene, which represents a remarkably high-yielding supramolecular design for ternary cocrystallisation. Cocrystallisation *via* directional C–I···π halogen bonds is also applicable to metal–organic halogen-bonded (MOXB)[124] cocrystals. An early report by Lapadula and co-workers presented cocrystals of Ni(II) and Co(II) dibenzoylmethanates with morpholine- or thiomorpholine ligands in the axial positions of the octahedrally-coordinated metal ions, wherein metal–organic units are interconnected into chains through a combination of C–I···π and either C–I···O or C–I···S halogen bonds.[125] More recently, the Frontera and Kukushkin groups reported the cocrystallisation of platinum "half-lantern" complexes through a combination of C–I···Pt, as well as C–I···π halogen bonds.[126]

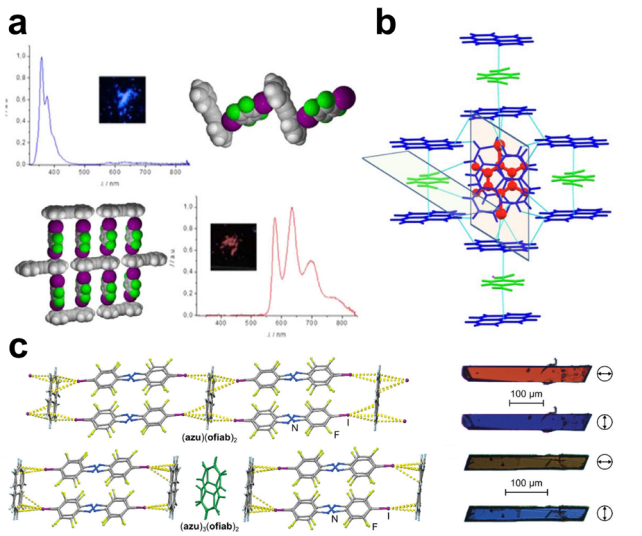

Fig. 6 (a) Stoichiomorphic cocrystals of tolane and **14tfib** exhibiting fluorescent and phosphorescent behaviour (adapted with permission.[123] Copyright 2015, American Chemical Society). (b) Ternary cocrystal of **14tfib**, pyrene and 1,4-dinitrobenzene based on C–I···π XBs and polar···π stacking (adapted with permission.[118] Copyright 2021, Wiley). (c) The XB ladder motif and images of pleochroic behaviour for cocrystals of azulene with an azobenzene-based halogen bond donor (adapted from ref. 127).

Crystal engineering of optical properties using halogen bonding to PAHs

The ladder-like C–I···π supramolecular synthon can be sufficiently reliable to support the design of materials with specific properties. This was illustrated through targeted synthesis of dichroic and pleochroic cocrystals[127] starting from the ladder-like structure of the previously reported **14tfib** cocrystal with naphthalene as a blueprint.[112] In the first instance, replacing the optically transparent PAH acceptor naphthalene with the blue chromophore azulene gave a material based on an identical ladder-like halogen-bonded architecture, wherein parallel alignment of all azulene rungs led to dichroic behavior, Next, replacement of the optically transparent **14tfib** rungs with the elongated azobenzene-based red chromophore **ofiab** produced a structure in which all red azobenzene chromophores are aligned in parallel, and perpendicular to the blue azulene ones (Fig. 6c). As a result, the cocrystal exhibited pleochroic

behaviour, which was evident from colour of the crystal changing from blue to red upon rotation in plane-polarised light.[127]

Due to the presence of heavy-atom halogens, the cocrystals exhibiting the ladder motif have also been investigated for the generation of phosphorescent materials, as already noted for tolane cocrystals reported by d'Agostino and co-workers.[123] In the context of PAHs, the Jin group demonstrated organic room-temperature phosphorescence emission[128] from cocrystals with naphthalene,[112] phenanthrene,[112] or other emissive aromatic XB acceptors, such as carbazole, fluorene, and pyrene (Fig. 5).[105,106,109] Similar behavior was also noted in cocrystals of **14tfib** with anthracene,[129] pyrene and coronene,[114] exhibiting a maximum average emission lifetime of 4.2 ms. In a similar vein, Abe *et al.*[130] have examined molecular doping in cocrystals assembled through C–I···π halogen bonds as a method to control organic phosphorescence. Using the cocrystal of **14tfib** and phenanthrene as a structural template, doping of pyrene molecules led to a mixed cocrystal of composition (**phen**)$_x$-(**pyr**)$_{1-x}$(**14tfib**)$_2$ composition, where varying the ratio of **phen** to **pyr** produced higher photoluminescence quantum yields (PLQY) of $>20\%$ and longer emission lifetimes (2.6 ms) through suppression of non-radiative decay pathways. Additional enhancement of phosphorescence emission was achieved by using deuterated **pyr** as a dopant, leading to PLQY of *ca.* 27% and emission lifetime of 4 ms. The C–I···π ladder motif is therefore tolerant to changes in PAH identity, as well as to sub-stoichiometric variation in cocrystal composition.

Targeting "latent" carbon

Hydrogen bonding has long been a crucial tool for cocrystal design, able to reliably engage a variety of heteroatom-based functional groups, such as carboxylic acids, amides and

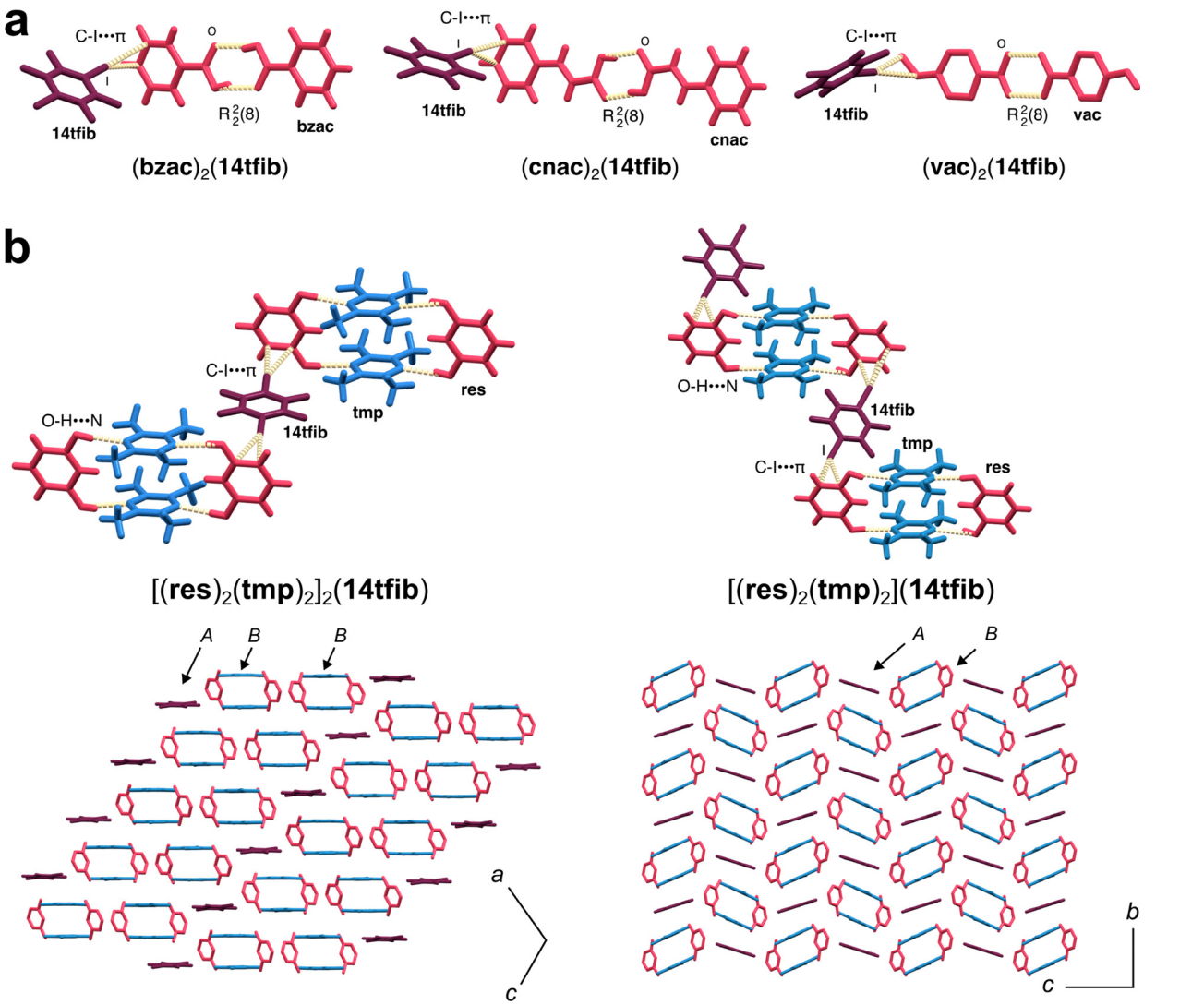

Fig. 7 (a) Cocrystals of **14tfib** and carboxylic acids, containing carboxylic acid dimers and C–I···π XBs (adapted from ref. 133, under the terms of the CC-BY license). (b) Stoichiomorphic ternary cocrystals of resorcinol, tetramethylpyrazine and **14tfib**, containing O–H···N HBs and C–I···π XBs (adapted from ref. 133, under the terms of the CC-BY license). Abbreviations **bzac**, **cnac**, **vac**, **res**, and **tmp** represent benzoic acid, cinnamic acid, vinylbenzoic acid, resorcinol, and tetramethylpyrazine, respectively.

hydroxyl groups.[131] In contrast, carbon-based aromatic moieties are generally poor HB acceptors[132] and, consequently, are usually not considered for molecular recognition when designing HB cocrystals. A cocrystal design strategy aimed towards engaging this ''latent'' aromatic carbon[133] using directional halogen bonds was recently demonstrated, leveraging the orthogonality of halogen and hydrogen bonds to target π-systems as XB recognition sites without disrupting the underlying HB motifs.

As an example of this hierarchical strategy, introduction of a halogen bond donor such as **14tfib** or 1,4-dibromotetrafluorobenzene (**14tfbb**) permitted the formation of binary cocrystals with benzoic acids, benzamide and phenols. The supramolecular structures based on common hydrogen-bonded homosynthons, such as the carboxylic acid dimers, benzamide ladder and phenol helices are retained, but are re-positioned in space through the formation of C–X···π (X = Br, I) halogen bonds to aromatic residues (Fig. 7a). Importantly, this hierarchical strategy was also applicable for the synthesis of ternary cocrystals, by using halogen bond donors to target the aromatic residues on robust and more complex hydrogen-bonded heterosynthon architectures, such as the phenyl moieties on a trimeric assembly of oxalic acid and benzamide held *via* acid-amide $R_2^2(8)$ synthons, or the aromatic rings of the resorcinol components in tetramolecular MacGillivray-type[134] assemblies of resorcinol and tetramethylpyrazine. In each case, the use of halogen bonding to carbon-only π-systems led to structures in which heteromolecular self-assembled structures typically found in simpler, binary hydrogen-bonded cocrystals were effectively used as building blocks for the formation of an even more complex three-component solid-state material. This is particularly evident in case of halogen bonding to the MacGillivray-type $(resorcinol)_2(tetramethylpyrazine)_2$ units, which yielded two stoichiomorphic cocrystals in which the tetramers were organised in different ways (Fig. 7b). The importance of hierarchical relationship between stronger hydrogen-bonded synthons and weaker C–X···π interactions was supported by periodic DFT calculations. The formation of the ternary cocrystal $(benzamide)_2$(oxalic acid)(**14tfib**) was possible mechanochemically from either pre-made $(benzamide)_2$(oxalic acid) cocrystal and **14tfib**, or from the pre-made $(benzamide)_2$(**14tfib**) with oxalic acid, demonstrating two different synthesis pathways that manipulate a different type of interaction. Feld and co-workers have demonstrated applicability of this strategy to **14tcib** as the XB donor.[135] In a similar vein, cocrystallisation of methyldiphenylphosphine oxide with bromine- or iodine-based XB donors yielded cocrystals comprised of hydrogen-bonded chains identical, or very similar, to those in the pristine solid phosphine oxide, but now cross-linked by C–I···π and C–Br···π interactions.[136] Halogen bonding to π-systems on hydrogen-bonded assemblies is also of broader relevance for studies of protein folding and protein–ligand interactions,[137] suggesting that cocrystals of this type might become of value as models when investigating more complex (bio)molecular recognition events.

Triple bonds and carbon lone pairs as XB acceptors

Compared to aromatic rings, using discrete C=C or C≡C moieties as XB acceptors in cocrystallisation is less explored. Nevertheless, overviews of the CSD indicated that halogen bonding to these, and other types of carbon-based moieties involving π-electrons, exhibits potential for directional assembly in the solid state (Fig. 8a).[97,114] As an example, Torubaev and Skabitsky recently demonstrated several cocrystals assembled through C–I···π XBs to acetylene moieties.[138] Specifically, the cocrystal of tolane as the XB acceptor and diiodoacetylene as the donor was found to assemble primarily through C–I···π halogen bonds to C≡C fragments, forming 1D halogen-bonded chains (Fig. 8b). In contrast, cocrystallisation of tolane with **14tfib** was previously reported to lead to formation of halogen bonds to the phenyl ring π-system, while the use of 1,3-diiodotetrafluorobenzene (**13tfib**) as the XB donor produced a cocrystal exhibiting a combination of C–I···π halogen bonds to the C≡C moiety and to the phenyl group of tolane. The comparison of these results suggests that C–I···π halogen bonds to acetylene groups are more sensitive to the size and shape of XB donors than halogen bonds to arene π-systems, possibly due to the smaller contact area of the acetylene π-system imposing greater geometric restrictions on XB formation. The formation of halogen-bonded complexes with alkene and alkyne π-systems is relevant to the mechanistic understanding of organic reactions, illustrating how site-specific recognition on carbon moieties can translate into chemical functionalisation.[139]

Individual carbon atoms have only recently been explored as single-point acceptors of halogen bonds, similar to, for example, nitrogen atoms in nitriles.[140–143] In particular, Mikherdov *et al.*[140] reported that cocrystallisation of mesityl isocyanide with different iodinated halogen bond donors, obtainable either by solution crystallisation and/or mechanochemistry produces two-component crystals in which the isocyanide moiety acts as a XB acceptor (Fig. 8c), with I···C contact distances ranging from 3.03–3.86 Å and with C–I···C angles from 131–179°.

Theoretical calculations indicate that such C–I···C halogen bonds are greatly supported by charge transfer between the isocyanide and halogen moieties through lp(C) → σ*(I–C) and lp(I) → σ*/π*(N≡C) donation, which is reminiscent of π-backbonding found in organometallic complexes. Notably, such charge transfer effects are less pronounced in nitrogen- or oxygen-targeting halogen bonds, demonstrating how using the carbon atom as a single-point XB acceptor might lead to unique opportunities in crystal engineering. Such cocrystals immediately offered an elegant application for reducing the odor of isocyanide reagents, with a demonstrated ≈50-fold decrease in isocyanide vapor in equilibrium with the solid cocrystal in comparison to the pristine isocyanide solid.

Finally, an almost completely unexplored class of XB acceptors are carbenes. In 1991, Arduengo *et al.*[144] reported a 1 : 1 stoichiometry adduct between a nucleophilic carbene and iodopentafluorobenzene (**ipfb**), representing a halogen-bonding interaction to an electron-deficient carbon atom (Fig. 8d). At room temperature, the adduct is in equilibrium with free carbene and **ipfb** in solution, demonstrating the labile nature of the C–I···C interaction. While cleavage of the C–I bond is observed over several hours in solution, the adduct is found to be stable in crystalline form. The exact nature of this

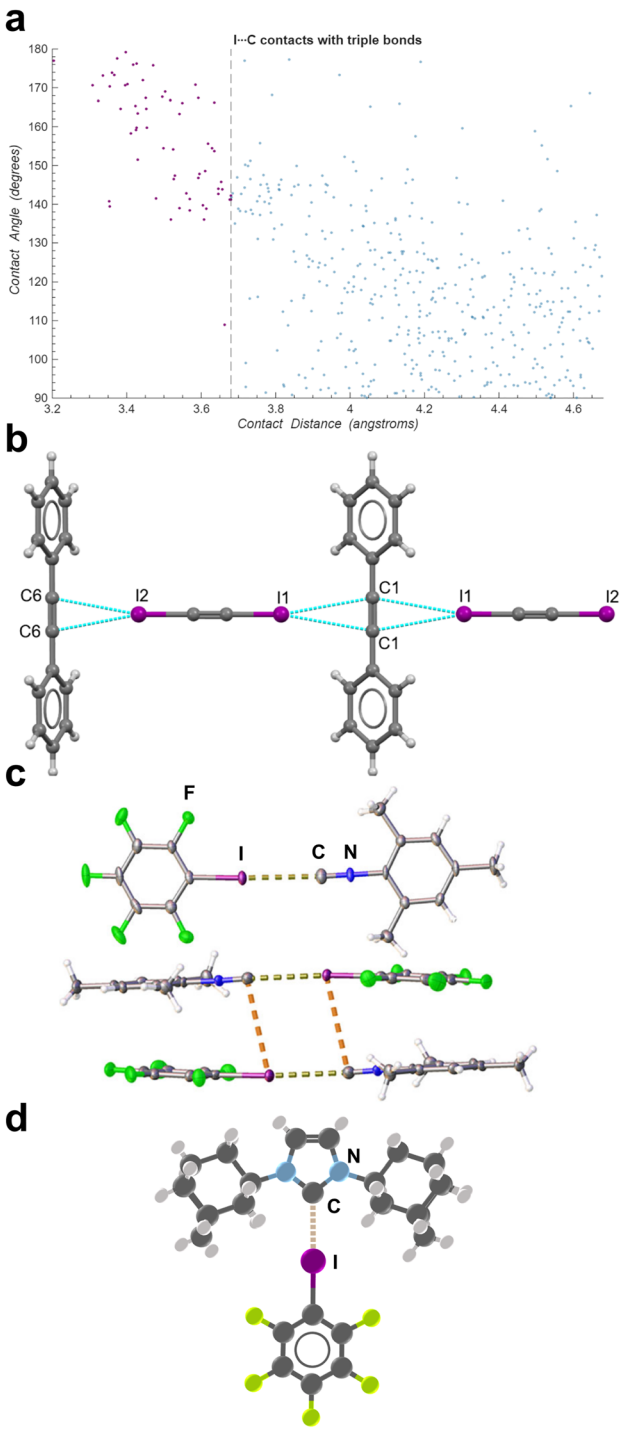

Fig. 8 (a) CSD search results demonstrating a preference for directionality of I···C short contacts (reproduced from ref. 114). (b) Cocrystal of 1,2-diiodoacetylene and tolane (adapted with permission.[138] Copyright 2024, American Chemical Society). (c) Cocrystal of iodopentafluorobenzene and mesityl isocyanide (adapted from ref. 140, under the terms of the CC-BY license). (d) Visualization of an iodopentafluorobenzene-carbene adduct.[144]

C–I···C interaction is still unclear, and recent theoretical calculations indicate this halogen bond may possess significant covalent character.[140] To the best of our knowledge, no other such halogen bonds to carbenes have been reported.

Cocrystals of C_{60} and other fullerenes

The concept of supramolecular recognition on carbon is strikingly demonstrated in case of cocrystals of fullerenes which, by definition, represent cocrystals with carbon in elemental form. Whereas cocrystals are known for other elements in molecular form, such as P_4 or S_8, the latter also known to form cocrystals with C_{60},[145] such examples are dwarfed by the number and compositional diversity of cocrystals involving fullerenes, providing another way in which the supramolecular chemistry of carbon is unique. To illustrate this point, the CSD contains 54 multi-component structures with S_8 molecules (of which 26 also contain a fullerene), whereas in case of C_{60} and C_{70} the numbers are 734 and 209, respectively.[146] The variety of molecules reported to form cocrystals with fullerenes is extensive, including interstitial inclusion compounds with small guest molecules like CH_4.[147] Therefore, the herein covered examples are meant to provide only a succinct but general overview of categories of coformers to which a crystal engineer may turn in cocrystal design.

Early research into fullerene cocrystallisation has focused on flexible, container-like molecular units, such as calixarenes, with the aim to accommodate the size and curved surfaces of fullerenes. The Atwood and Raston groups focused on calixarenes as reagents for cocrystallisation of fullerenes demonstrating, for example, the use of calix[8]arenes for separating C_{60} from C_{70}.[148,149] The aromatic cavities and the conformational flexibility of calixarenes were found to offer a suitable molecular platform for establishing heteromolecular π···π interactions with fullerenes in the solid state (Fig. 9a). In another example of a container-like molecule, Steed *et al.*[150] reported that the bowl-shaped cyclotriveratrylene (**CTV**) molecule could lead to formation of ball-and-socket complexes in the solid state, where the C_{60} represents the ball and **CTV** provides a socket (Fig. 9b). The contacts between the **CTV** and C_{60} units were found to be within the van der Waals radii expected for non-bonded carbon-carbon contacts, with the C_{60} unit being fully ordered in the concave face of **CTV**. Makha *et al.*[151] demonstrated a profound influence of substituents on the structure of cocrystals of calixarenes and fullerene: whereas calix[6]arene was found to form a 1 : 2 stoichiometry complex with C_{60},[152] with a crystal packing exhibiting a 3D array of fullerene units, using *p*-benzylcalix[6]arene led to a solid-state complex of 1 : 3 stoichiometry, with C_{60} units now exhibiting an overall honeycomb-like arrangement throughout the crystal. Although both cocrystals are primarily assembled *via* similar π···π and C–H···π interactions, conformational flexibility and variations in the choice of sidearm units leads to very different packing arrangements.

Coformers with molecular curvature

Aromatic coformers exhibiting molecular curvature have also been effectively exploited in designing cocrystals with fullerenes,[153] with the curvature of the coformer aromatic surfaces thought to enhance the compatibility of π-areas. Such molecular scaffolds include corannulene,[154–157] azacorannulenes,[158,159] and triquinacenes,[160–162] among others,[163] which have been used as

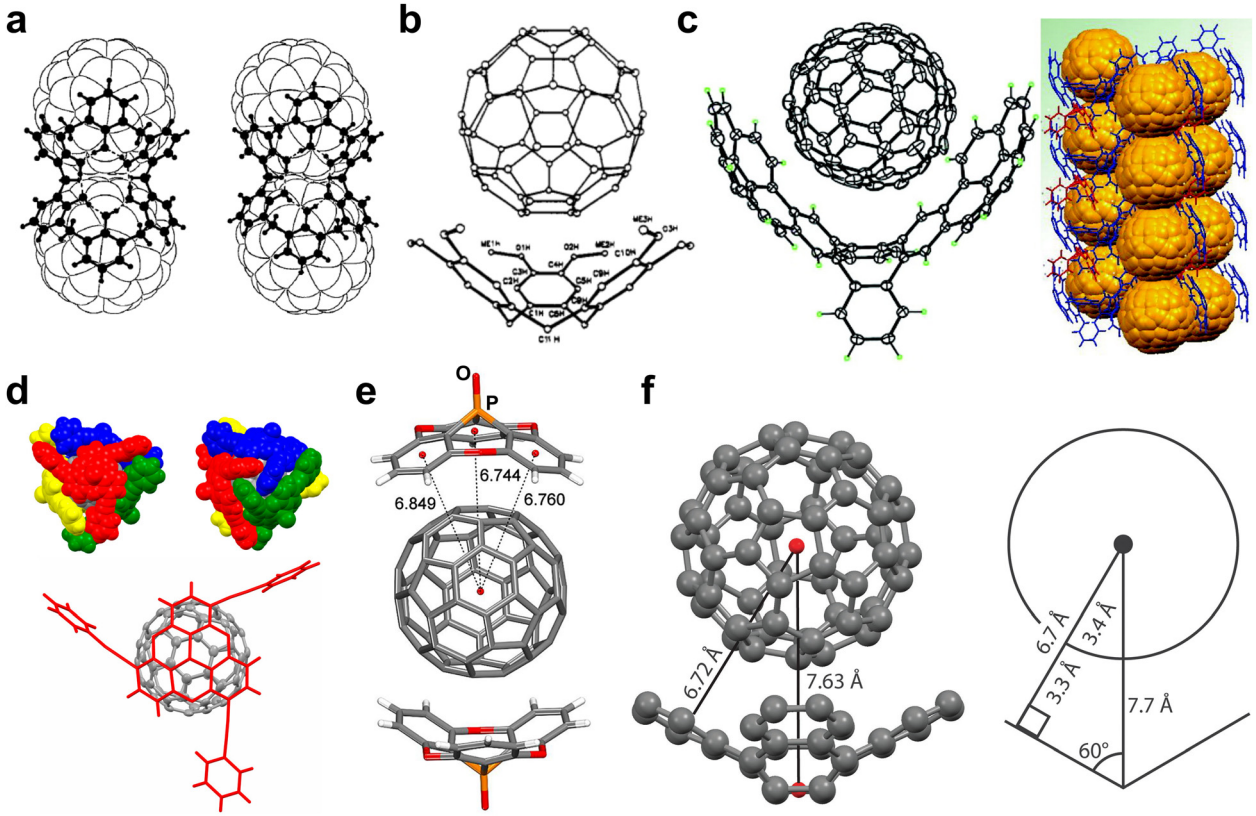

Fig. 9 (a) Calix[6]arene assemblies with C_{60} (left) and C_{70} (right) (adapted with permission.[152] Copyright 1998, Wiley) (b) Assembly of bowl-shaped CTV with C_{60} (adapted with permission.[150] Copyright 1994, American Chemical Society). (c) Buckycatcher assembly with C_{60} and crystalline packing (adapted with permission.[164] Copyright 2007, American Chemical Society). (d) C_3-symmetric phosphangulene encapsulation of C_{60} (adapted with permission.[166] Copyright 2014, American Chemical Society). (e) Double-capped assembly in cocrystal of phosphangulene oxide and C_{60} (adapted with permission.[168] Copyright 2019, American Chemical Society). (f) A model structure and diagram for the sphere-in-a-cone model of C_{60} binding (adapted from ref. 171).

coformers on their own or have been incorporated into highly-specified fullerene binders. An example of the latter is the "Buckycatcher", reported in 2007 by Sygula *et al.*[164] The "Buckycatcher" molecule was explicitly designed for complexation with C_{60} through two corannulene pincers attached to a tetrabenzocyclooctatetraene core that can grip the C_{60} *via* concave–convex π···π interactions (Fig. 9c).

A class of conical aromatic molecules that were found to be particularly well-suited for cocrystallisation with fullerenes are phosphangulenes,[165] with Yamamura *et al.*[166] reporting a C_3-symmetric chiral phosphangulene with phenylacetylene appendages capable of forming a supramolecular capsule around a C_{60} molecule. In the resulting cocrystal, C_{60} interacts *via* concave–convex interactions with four phosphangulene cores, wrapped together *via* C–H···π interactions of the phenylacetylene groups (Fig. 9d). The Wuest group has shown how "awkwardly-shaped" phosphangulene derivatives can be made, with structures that hinder strong homomolecular stacking interactions between phosphangulene units and promote heteromolecular interactions with curved fullerene surfaces instead.[167] For example, phosphangulene chalcogenides are found to exhibit more acute cone angles in comparison to regular phosphangulene, enhancing the ability to interact with C_{60} and C_{70}.[168–170] Intermolecular π···π stacking leads to fullerenes singly- or doubly-capped by phosphangulene chalcogenides (Fig. 9e), the latter being arranged either directly across the fullerene or rotated *ca.* 90° relative to each other along the fullerene surface.

King *et al.*[171] proposed a sphere-in-a-cone model to estimate the effectiveness of binding between curved molecules and C_{60}, using the contact area between the two components (Fig. 9f). The cone angle of the curved aromatic (θ) and the radius of C_{60} (R) are used to derive the contact circumference as $2\pi r$, where $r = R\cos\theta$. By comparing the contact area values derived from the geometric equation, this model is shown to reproduce the difference in theoretical binding energies between a corannulene-C_{60} complex and quadranullene-C_{60} complex. Although binding energies in solution or in gas-phase calculations do not necessarily correlate with crystallisation behaviour, this model nevertheless offers a way to investigate molecular compatibility prior to more costly synthesis and cocrystallisation studies.

Coformers with molecular flexibility

Beyond molecular curvature, another approach for solid-state complexation of fullerenes is based on flexible molecular systems, allowing for malleable π-surfaces which can adjust for optimal binding.[172,173] For example, Tang *et al.*[174] reported a flexible, triptycene-based nanocarbon system that interconverts

between two different curved conformations, termed the propeller and the tweezer, capable of forming cocrystals with C_{60} and C_{70}. The pristine nanocarbon crystallises in the propeller conformation, but is found in the tweezer conformation in both cocrystals, binding the fullerenes through π···π interactions within the tweezer cavity. Another fullerene molecule is also found sandwiched between two adjacent nanocarbons, demonstrating a second form of fullerene binding in both cocrystal structures. Calculations indicate that the tweezer binding for C_{60} is 3.12 kcal mol^{-1} more favorable than binding by divergent blades (5.22 kcal mol^{-1} for C_{70}), a difference that appears to be ultimately related to a better shape match between the components, and increased van der Waals interactions.

He *et al.*[175] reported nanographene-based molecular tweezers for binding C_{60} in the solid state, comprising two hexabenzocoronene units connected through a twisted carbaporphyrin or a BF_2-porphyrin, that aligns the mean planes of the hexabenzocoronene units at angles of 30.5° and 35.2°, respectively. Crystallisation of such molecular tweezers in the presence of C_{60} led to cocrystals of 1 : 1 stoichiometry, with C_{60} units bound by the tweezers through π···π interactions (Fig. 10a). Crucial for this binding is the ability to distort the molecular tweezers for accommodating C_{60}, with the mean planes of the hexabenzocoronene units now at 47.8° and 45.0°, respectively.

Porphyrins as coformers

Porphyrinoids can be effectively used for solid-state, stacking-based recognition with fullerene molecules,[176] as illustrated by Boyd *et al.*[177] who reported a series of cocrystals containing tetraphenylporphyrins and either C_{60} or C_{70}, assembled *via* π···π interactions (Fig. 10b). In the cocrystals, C_{60} was consistently found placed above the electron-rich porphyrin cores, with distances between the fullerene and the mean plane of the porphyrin system being in the range 2.7–3.1 Å. Similar motifs were also found with C_{70}, with the longer axis of the fullerene oriented towards the porphyrin face. This early report stresses the relevance of porphyrin planarity for fullerene recognition through interactions between flat and convex surfaces. This is worth highlighting as the molecular curvature is seen as being of paramount importance for successful complexation with convex fullerene surfaces.[178,179] The recognition of fullerenes by porphyrin moieties is tolerant to presence of metals, providing an opportunity for creation of more complex materials through modification of porphyrin cores by metal binding. Such tolerance was shown by Olmstead *et al.*[180] for a series of fullerene cocrystals with metal-containing octaethylporphyrin (OEP) units. Possibly due to the combination of bulky fullerenes and large, planar porphyrins leading to less than effective crystalline packing, solvent inclusion in such cocrystals is common (Fig. 10c). The impact of the crystallisation solvent on the porphyrin···C_{60} cocrystals was investigated more recently by Roy *et al.*,[181] who demonstrated solvent choice as the determining factor affecting cocrystal composition, rather than solution stoichiometry of molecular components, *i.e.* the same solvent was found to always produce the same crystalline form. Furthermore, cocrystals appear to always contain one type of

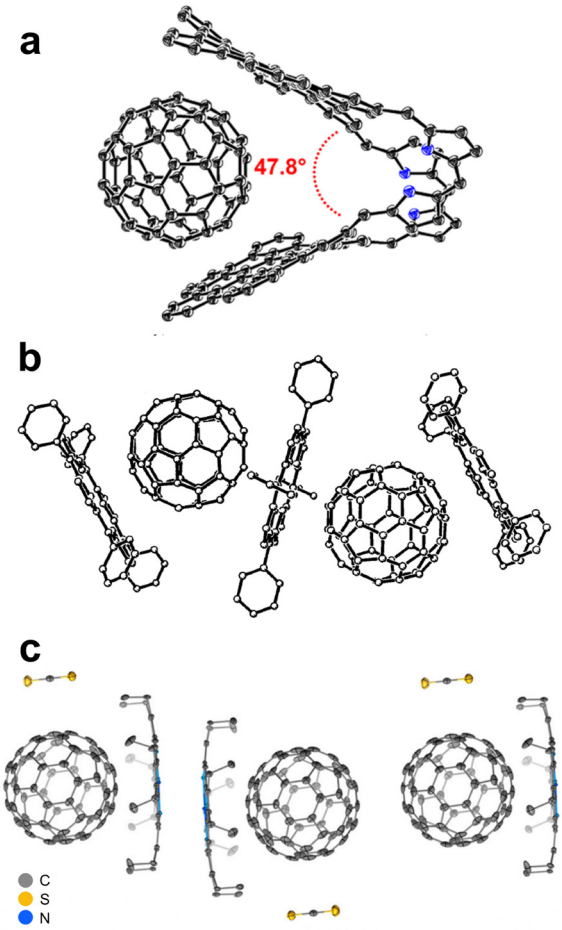

Fig. 10 (a) C_{60} bound by hexabenzocoronene-based molecular tweezers (adapted with permission.[175] Copyright 2024, American Chemical Society). (b) Stacking motif in a cocrystal of tetraphenylporphyrin and C_{60} (adapted with permission.[177] Copyright 1999, American Chemical Society). (c) Stacking motifs in the cocrystal of Co^{II}(OEP), C_{60}, and CS_2 (adapted with permission.[181] Copyright 2020, American Chemical Society).

solvent even when grown from a mixed solvent environment, indicating a highly selective crystallisation process involving solvent discrimination. Although this work directly investigated solvent effects in porphyrin-based cocrystals, it also highlights a more general cocrystal design issue encountered when using large, aromatic molecules: individual interactions between π-surfaces can lead to predictable assemblies, however the manner in which the resulting self-assembled units arrange in the solid state is less predictable and/or controllable. In many of the herein discussed examples, cocrystals with C_{60} contain solvent molecules within the structure, yet the impact of these solvent molecules is rarely discussed in relation to crystal packing motifs.

Different approaches to fullerene cocrystallisation

One so far poorly explored cocrystal design approach is the use of flexible phenyl substituents[182] or adaptable hydrogen-bonding networks[183] to encapsulate fullerenes through π···π interactions. An elegant example of such a strategy is the

cocrystal of C_{60} with phenol,[183] based on hydrogen-bonded phenol architectures encapsulating each C_{60} molecule *via* four π···π interactions. The phenol rings and the neighboring C_{60} surface are nearly co-planar, maximising the overlap of π-systems, while the phenol molecules are mutually linked through O–H···O hydrogen bonds. Recently, Wang *et al.*[184] reported cocrystallisation with C_{60} as a method to crystallise tetraphenyltin-cluster compounds, which are otherwise obtained as amorphous solids in their pristine state. A "π-trap" approach was employed, focusing on the stacking interactions between phenyl groups and C_{60} to guide self-assembly (Fig. 11a). This approach was then further generalised by using C_{70} and endohedral $Lu_3N@C_{80}$ as coformers with tetranaphthyltin-cluster compounds, demonstrating how cocrystallization with fullerenes can be used to isolate normally-amorphous solids in a crystalline environment, reminescent of the molecular sponges approach[185] as well as other reports where cocrystallisation is used to obtain molecules in crystalline form that are otherwise difficult to crystallise.[186–188]

A recent example of cocrystal design based on C–H···π interactions was reported by Yamamoto *et al.*,[189] who described the synthesis of an anthracene-based macrocycle with a central cavity capable of binding C_{60}, forming a so-called "nano-Saturn" complex (Fig. 11b). The cavity exhibits 18 inward-directed C–H bonds, with a cavity diameter of 1.03 nm when accounting for van der Waals radii of hydrogen (1.2 Å). The macrocycle was found to form a cocrystal with C_{60}, where each fullerene molecule is bound in the centre of the cavity. Theoretical calculations indicated a total macrocycle···C_{60} binding energy of *ca.* −57 kJ mol^{-1}, comparable to a hydrogen bond of intermediate strength.[190] A similar "nano-Saturn" complex was also reported with C_{70}, demonstrating cocrystallisation with an ellipsoidal coformer, and the design was also extendable to more strongly binding nanocages.[191]

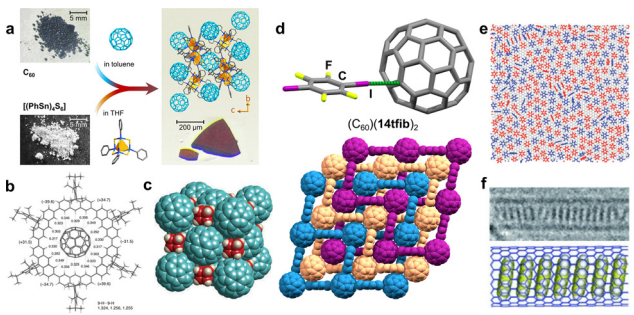

Fig. 11 (a) π-trap approach for crystallizing normally-amorphous tetraphenyltin-cluster compound (adapted from ref. 184 under the terms of the CC-BY license). (b) A nano-Saturn complex assembled through C–H···π interactions (adapted with permission.[189] Copyright 2018, Wiley). (c) Crystalline packing of the (C_{60})(cubane) cocrystal (adapted with permission[192] from SNCSC). (d) Cocrystal of C_{60} and **14tfib**, assembled through C–I···π XBs (adapted from ref. 114). (e) Monolayer of benzene (red) and hexafluorobenzene (blue) on a graphene surface (adapted with permission.[198] Copyright 2012, American Chemical Society). (f) Coronene stack inside a carbon nanotube (adapted with permission.[201] Copyright 2011, Wiley).

Shape-based cocrystallisation of fullerenes and cubane was investigated by Pekker *et al.*,[192] demonstrating temperature-dependent orientational ordering and topochemical reactivity. The cocrystal (C_{60})(cubane) is assembled into a face-centered cubic structure at room temperature, structurally-similar to the pristine structure of C_{60}, with ordered cubane units sitting in octahedral voids between rotationally-disordered C_{60} units (Fig. 11c). Below 140 K, both C_{60} and cubane are orientationally-ordered, while from 140–470 K, cubane units are static and C_{60} units are rotationally-disordered. Above 470 K, covalent bond formation between cubane and C_{60} is observed, yielding C_{60}-cubane polymers as amorphous solids. Similar temperature-dependent behavior was also observed in a (C_{70})(cubane) cocrystal,[192] leading to many further studies of the pressure- or temperature-related dynamic properties of both cubane-containing cocrystals.[193,194]

Cocrystallisation of C_{60} was also accomplished through directional interactions, by halogen bonding. For example, a recent report[114] identified the formation of a halogen-bonded cocrystal of composition (C_{60})(**14tfib**)$_2$, with a structure composed of three interpenetrated networks of square-grid (sql) topology, held through C–I···π halogen bonds with each C_{60} unit acting as a four-fold node, and **14tfib** molecules acting as linkers (Fig. 11d). Notably, the C–I···π distances of 3.55 Å are the shortest directional interactions to the C_{60} units in the cocrystal, with separations between individual fullerene units being in the range 3.42–3.46 Å, which is above the van der Waals contact distance of 3.4 Å. Other cocrystals based on halogen bonding to fullerenes have been reported,[195] notably (C_{60})(**135tftib**) and $(C_{70})(I_2)$ described by Zhang *et al.*[196] and Ghiassi *et al.*,[197] respectively, indicating that halogen bonding to carbon-only curved surfaces may offer a different approach to fullerene recognition outside of the more common stacking approaches.

Carbon nanostructures: a new frontier

Whereas research on carbon nanostructure materials typically focuses on covalent structures, such as graphenes, carbon nanotubes (CNTs), nanohorns, *etc.*,[198] the concepts outlined for cocrystallisation of fullerenes or PAHs have also found use in the context of such nanomaterials. An example is the concomitant assembly of benzene and hexafluorobenzene on graphene surfaces (Fig. 11e), leading to oriented growth of (benzene)(hexafluorobenzene) stacks based on phenyl···perfluorophenyl motifs.[199] In the context of CNTs, Matsuno *et al.*[200] have described a cocrystal involving a tubular macrocycle and corannulene, in which the corannulene units are held in the macrocycle cavity through C–H···π interactions.

The corannulene units in this complex, which effectively represents an inversion of the already mentioned nano-Saturn design[189] for fullerene binding, were found to rotate freely along the central tube axis due to the curved interior of the macrocycle, enabling the weak C–H···π interactions to relay across the curved surface. Similar behaviour could, in principle, be extended to the inclusion complexes involving curved inner surfaces of CNTs, which were previously shown to uptake

coronene molecules and generate 1D stacks of PAHs propagating along the nanotube length (Fig. 11f).[201] Supramolecular derivatisation of CNTs is a well-developed area, where π···π interactions play a significant tole, involving either small molecules or polymers as derivatisation agents.[202] For example, the solubility of single-walled carbon nanotubes (SWCNTs) in water was found to significantly increase in the presence of cationic surfactants bearing PAH substituents,[203] capable of engaging in π···π interactions with the curved nanotube surface, producing aqueous polyelectrolytes. Such non-covalent structures were exploited to develop water-soluble complexes capable of photo-induced charge transfer, combining SWCNTs[204] bearing cationic pyrene surfactants as electron acceptors, and anionic metal porphyrins as donors, as demonstrated by Guldi *et al.*[205] By using a fullerene- and pyrene-substituted cationic surfactant, this concept was deployed for assembling an intrinsically interesting complex of three carbon-based species: a PAH, a fullerene and a CNT.[206]

C–H···π interactions

The C–H···π interaction is an important cornerstone of aromatic molecule crystallisation.[207] For example, C–H···π interactions function alongside slip-stacking of π-systems to assemble neutral, planar, aromatic molecules, such as PAHs, into herringbone motifs.[208] A well-known solid-state structural motif involving multiple C–H···π interactions is the phenyl embrace, involving molecules with arylated surfaces.[209] The phenyl embrace, recognised in 1995 by Dance and Scudder,[210] can be found in crystal structures containing diverse pyramidally- or tetrahedrally-shaped species such as trityl groups, triphenylphosphine, tetraphenylphosphonium cations, metal complexes with peripheral aromatic units, and was observed in cocrystals involving additional hydrogen or halogen bonds.[211] Theoretical studies have shown that C–H···π interactions are dominated by dispersion contributions,[212] differentiating them from traditional hydrogen bonds which possess large electrostatic contributions. This distinction, however, becomes somewhat dubious when considering saturation of the carbon atom. Carbon saturation directly influences the acidity of the hydrogen atom,[213] leading to larger expected electrostatic contributions for C–H···π interactions as the type of the C–H hydrogen bond donor changes in the order $C(sp)$–H > $C(sp^2)$–H > $C(sp^3)$–H. The C–H···π interactions are also of considerable significance in structural biology, playing an important role in protein folding and molecular recognition.[214] Cocrystallisation can be seen as a suitable proxy to study biological recognition based on C–H···π interactions prior to potentially more demanding *in vitro* or *in vivo* studies. In that context, cocrystallisation of steroids with arenes, illustrated in the following section, is an area in which small-molecule cocrystallisation studies advanced both the understanding of the structural complexity, as well as of the molecular recognition behavior, of important signalling molecules.

Selective recognition of PAHs by steroids

Cocrystallisation of steroids with substituted phenols, such as 4-bromophenol, was used in 1960s to facilitate structural analysis of such complex biomolecules using the heavy atom method,[215] and has also been of interest more recently as means to support determination of absolute configurations.[216] In a pioneering report of this non-covalent derivatisation approach, Eger and Norton[215] noted the formation of similar solid-state molecular complexes of steroids with non-substituted aromatic hydrocarbons such as naphthalene.[217] This observation inspired a subsequent systematic exploration of the ability of structurally different steroids progesterone (**pro**), pregnenolone, β-estradiol and estrone to form cocrystals with a range of aromatic and aliphatic molecules.[218] The study revealed a very high propensity of **pro** for cocrystallisation with aromatic coformers which, upon single crystal X-ray diffraction analysis, was found to rest on the formation of "sandwich" or "half-sandwich" structures based on parallel self-assembly of the steroid α-face with the arene π-surface (Fig. 12a). The formation of the sandwich assemblies was specific for **pro**, rationalised by the presence of a conjugated enone in the hydrocarbon skeleton of the steroid, providing the hydrogen atom-lined α-face of **pro** with a highly positive ESP (Fig. 12b), in that way generating a flat molecular surface which is well-suited for C–H···π interactions. Specifically, **pro** was found to cocrystallise with all 19 PAHs and substituted arenes in the initial set of 24 coformers, with all determined crystal structures exhibiting the α···π stacking motif, regardless of the presence of substituents on the arene.

In contrast, pregnenolone, β-estradiol and estrone exhibited a much lower cocrystallisation propensity with arenes, which was also not based on the α···π motifs. Specifically, β-estradiol formed cocrystals based on inclusion of suitably-sized arenes into the channels of a self-assembled hydrogen-bonded steroid framework (Fig. 12c).[219] While this hydrogen-bonded network is flexible and can accommodate a variety of PAHs, the shape and size of the coformer can dictate whether cocrystal formation is successful, as suggested by the fact that a β-estradiol cocrystal with 1,2-dimethylnaphthalene was readily isolated, but a cocrystal with non-substituted naphthalene was not observed. Estrone was found to form only one cocrystal in the entire screen, through π-stacking of the steroid phenol moiety with perfluoronaphthalene. A computational investigation by Luo *et al.*[220] demonstrated how the hydrogen bonding ability of steroids can directly influence the likelihood of forming a cocrystal: a comparison of **pro** and pregnenolone showed that the latter steroid is more stable as a pristine solid due to presence of O–H···O hydrogen bonds, which do not exist in solid **pro**. Consequently, whereas the structure of the steroid covalent backbone is likely to be crucial for enabling the α···π recognition motifs, it is also likely that optimising the functionalities at the steroid periphery is key for successful solid-state cocrystallisation with PAHs. This was highlighted by experimental studies on exemestane, an anti-cancer steroidal drug, which showed decreased α···π selectivity due to a conjugated dienone group in the steroid backbone.[221] The effect of the conjugated dienone moiety is two-fold: greater unsaturation reduces the number of C–H groups available for α···π motifs, while the presence of C=C bonds increases repulsion with electron-rich arene surfaces. Nevertheless, α···π assembly is

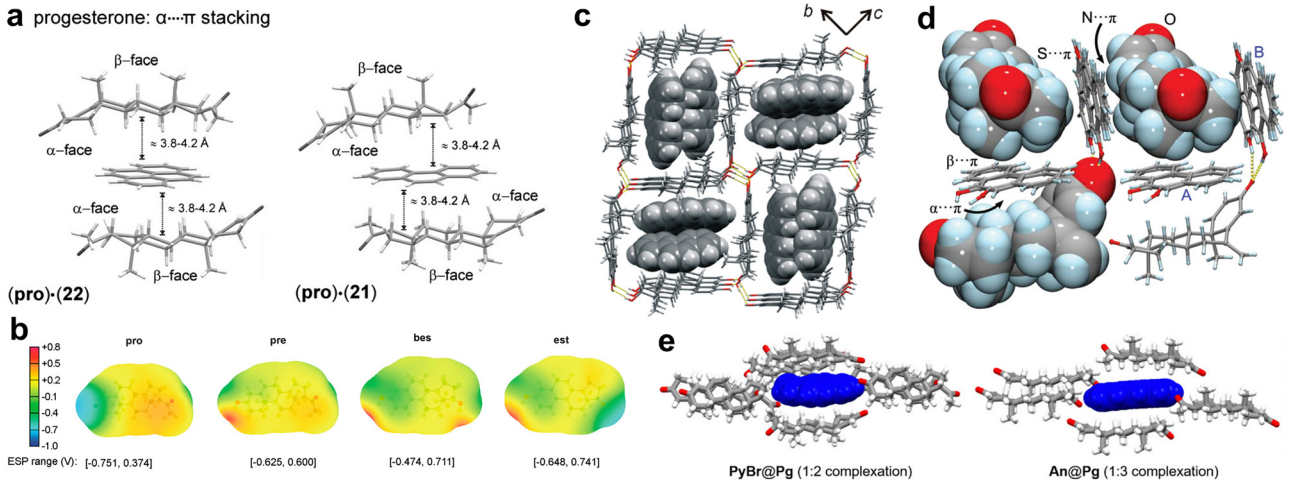

Fig. 12 (a) Illustration of the α···π recognition motif in progesterone–arene cocrystals (adapted with permission.[218] Copyright 2010, the authors). (b) ESP maps for progesterone, pregnenolone, β-estradiol, and estrone (adapted with permission.[218] Copyright 2010, the authors). (c) β-estradiol HB network with α···π recognition channels (adapted with permission.[219] Copyright 2015, American Chemical Society). (d) Varied C–H···π recognition motifs in an exemestane cocrystal (adapted with permission.[221] Copyright 2020, the authors). (e) α···π recognition motif in progesterone cocrystals exhibiting circularly polarised luminescence (adapted with permission.[223] Copyright 2022, American Chemical Society).

found in cocrystals with 9-hydroxyphenanthrene and with 1-hydroxypyrene, along with further β-face and side-on interactions between exemestane and the arene, presenting C–H···π as the dominant supramolecular motif in the cocrystal (Fig. 12d). The high propensity of **pro** for cocrystal formation with arenes could also be of biological relevance, as indicated by the structure of the DB3 antibody binding site exhibiting short contacts between the steroid unit and neighboring aromatic tryptophane units.[222]

The potential of the α···π recognition motif in creating functional materials was demonstrated by Wang *et al.*,[223] whose studies of chiroptical properties of **pro** cocrystals with arenes revealed the generation of circularly polarised luminescence and room-temperature phosphorescence. The chirality of the **pro** backbone provides a means to transfer chiral characteristics to the luminescence of arene coformers, such as pyrene and perylene, leading to luminescence disymmetry values (g_{lum}) on the order of 10^{-3}. The formation of the α···π sandwich motifs effectively isolates the arene subunits in the solid state (Fig. 12e), leading to cocrystal emission that closely resembles the emission of isolated arene monomers, distinct from the emission of the crystalline arenes. Additionally, cocrystallisation with **pro** was found to stabilise emissive triplet states of brominated PAHs by limiting non-radiative relaxation, leading to phosphorescence emission. The α···π recognition is also likely to have value in the context of pharmaceutical materials science, as demonstrated by higher dissolution rates of **pro** cocrystals over the solid steroid observed by Zeng *et al.*,[224] potentially opening new opportunities in the design of multicomponent pharmaceutical solids without strong hydrogen bonds.

Cocrystals based on C–H···π hydrogen bonding with acetylene donors

The C–H groups on acetylenic, sp-hybridised carbon atoms are well-suited for cocrystallisation involving C–H···π hydrogen bonds. An example is the cocrystal of two hydrocarbons, (acetylene)(benzene), described by Boese *et al.*[225] The acetylene and benzene moieties in the cocrystal are assembled into chains held by C–H···π hydrogen bonds, with acetylene as the donor (Fig. 13a). Within the chain, the acetylene units are positioned perpendicular to the centres of the neighboring benzene rings, with C–H···$ring_{centroid}$ distances of *ca.* 2.45 Å, calculated to correspond to an intermolecular interaction energy of −12.6 kJ mol^{-1}. The cocrystal was found to be stable under pressures of up to at least 28 GPa,[226] which is remarkable considering that pure acetylene is known to polymerise at pressures ≈3.5 GPa.[227] Such greatly improved pressure stability of acetylene in the cocrystal is rationalised by the alkyne moieties being effectively held in separation by the cocrystal framework.

These types of cocrystals, composed of different types of hydrocarbons, have attracted considerable attention in the context of extraterrestrial mineralogy.[228] Specifically, as both acetylene and benzene are expected to be found on Titan, it has been speculated that the (acetylene)(benzene) cocrystal could be observed as a naturally-occurring mineral in Titan lake evaporites,[229,230] representing an example of an extraterrestrial organic mineral.[231] Other Titan-relevant cocrystals based on simple hydrocarbons have been predicted or experimentally observed on Earth, including $(benzene)_3$-(ethane)[232] and (butane)(acetylene).[233] Kirchner *et al.*[234] have investigated a series of cocrystals containing acetylene as a hydrogen bond donor. In addition to more traditional hydrogen bond acceptors, such as ketones, pyridines, and nitriles, cocrystals were prepared in which acetylene forms directional interactions to π-systems of aromatic molecules, such as *m*-xylene and mesitylene, relying in each case on the appearance of C–H···π hydrogen bonds between cocrystal components.[235] In the structure of (acetylene)(*m*-xylene), each acetylene unit is found to form C–H···π hydrogen bonds to the π-system of *m*-xylene, as well as to the triple bond system of a neighboring acetylene moiety, resulting in a zig-zag chain of acetylene molecules decorated by *m*-xylene units.

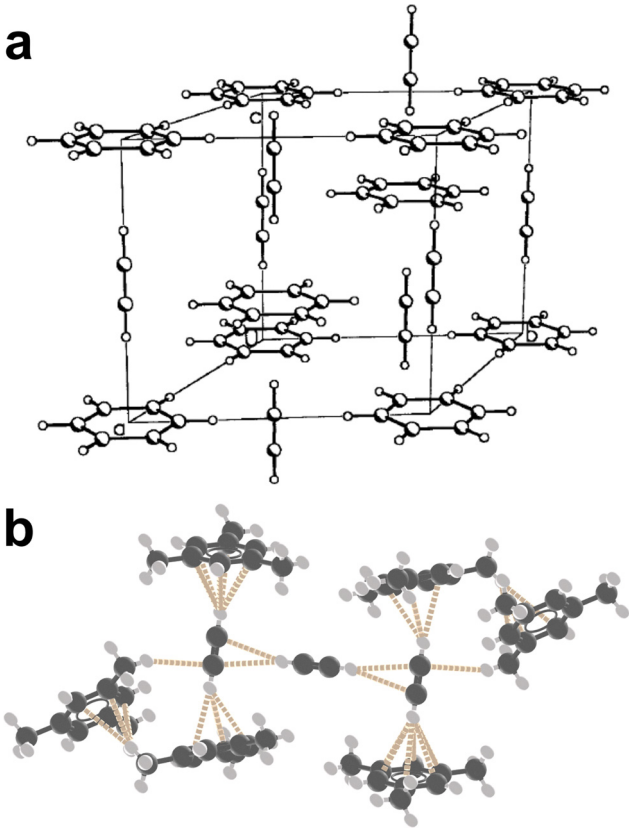

Fig. 13 (a) Structure of the cocrystal of acetylene and benzene (adapted with permission.[225] Copyright 2003, Wiley). (b) Structure of the cocrystal of acetylene and mesitylene.[234]

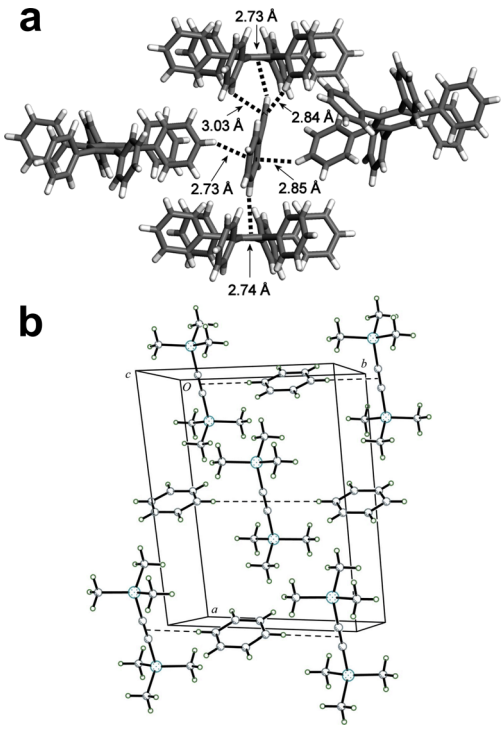

Fig. 14 (a) Structure of the cocrystal of hexaphenylbenzene and phenylacetylene (adapted with permission.[235] Copyright 2010, American Chemical Society). (b) Structure of the cocrystal of benzene and bis(trimethylsilyl)acetylene (adapted with permission[236] of the International Union of Crystallography).

In the (acetylene)(mesitylene)$_2$ cocrystal, the asymmetric unit contains three mesitylene molecules and 1.5 molecules of acetylene, where one acetylene unit forms C–H$\cdots\pi$ hydrogen bonds to two symmetrically-independent mesitylene moieties, while the remaining acetylene unit forms C–H$\cdots\pi$ hydrogen bonds to C$\equiv$C moieties of neighboring acetylene molecules (Fig. 13b). The third symmetry-independent mesitylene molecule is held in place through a combination of C–H$_{methyl}\cdots\pi$ interactions with other mesitylene and acetylene molecules, simultaneously acting as a C–H$\cdots\pi$ hydrogen bond donor and an acceptor.

Ethynyl moieties offer an easily installable functionality for enabling C–H$\cdots\pi$ interactions. One report examined the tendency of hexaphenylbenzenes to engage in C–H$\cdots\pi$ interactions with alkynes, with an ultimate aim towards developing organic acetylene sponges.[235] In addition to a series of single component crystals, the tendency of alkynes to engage in supramolecular interactions with π-systems was examined in a 2 : 1 respective stoichiometry cocrystal of hexaphenylbenzene with phenylacetylene, in which phenylacetylene molecules form C(sp)–H$\cdots\pi$ and C(sp^2)–H$\cdots\pi$ interactions with central rings of different hexaphenylbenzene units (Fig. 14a). Additionally, the phenylacetylene molecule is held in place by C(sp^2)–H$\cdots\pi$ interactions from adjacent hexaphenylbenzene units.

While the preceding examples highlight aromatic rings as acceptors of C–H$\cdots\pi$ hydrogen bonds, cocrystals have also been reported where benzene groups also act as C–H$\cdots\pi$ donors. As an example, Meyer-Wegner *et al.*[236] have reported the structures of two cocrystals, (bis(trimethylsilyl)acetylene)(benzene) and (diphenylacetylene)(benzene), where C–H$\cdots\pi$ interactions originate from C(sp^2)–H groups on the benzene units targeting both triple bonds and neighboring phenyl π-systems. In the former cocrystal, benzene is found to form highly linear C–H$\cdots\pi$ interactions to the acetylene moiety of bis(trimethylsilyl)acetylene (C–H$\cdots$C$=$C$_{centroid}$ = 3.013 Å), producing chains of benzene and bis(trimethylsilyl)acetylene units (Fig. 13b). In the (diphenylacetylene)(benzene) cocrystal, the benzene molecules form short C–H$\cdots\pi$ interactions to the phenyl rings of diphenylacetylene molecules, with each phenyl ring interacting with a benzene molecule on one side and another diphenylacetylene on the opposite side. This yields staircase-type chains of alternating benzene and diphenylacetylene molecules, with adjacent chains connect through diphenylacetylene-diphenylacetylene C–H$\cdots\pi$ interactions. It is noteworthy that the (diphenylacetylene)(benzene) cocrystal is assembled only through C–H$\cdots\pi$ short contacts and not π–π stacking, despite the formula unit containing three aromatic rings. The ability of C–H groups on PAHs to act as hydrogen bond donors in cocrystal formation is not limited to π-acceptors. This was shown in the pioneering work from the Jones group, who used C–H$\cdots$O motifs between anthracene and 3,5-dinitrobenzoic acid derivatives to construct binary cocrystals, in one case also isolating a ternary system involving anthracene and benzene as hydrogen bond donors.[237]

Menshutkin complexes and emerging interactions

Whereas halogen bonding is now a widely studied interaction, other σ-hole interactions are increasingly attracting attention as tools for cocrystal design.[238] Just as the removal of electron density along the σ-bond from a halogen atom can generate a σ-hole, the analogous effect along σ-bonds involving an atom of a chalcogen (Group VI), pnictogen (Group V), and a tetrel (Group IV) element can generate two, three, or four σ-holes, respectively.[239] While most examples of cocrystal design using chalcogen, pnictogen, and tetrel bonds focus on N,[240] O,[241,242] and halide anion[243] acceptors, interactions with carbon are beginning to be explored.

Heavy pnictogens and chalcogens have been observed to interact with π-systems, with such interactions present in a variety of single component crystal structures.[244,245] The Chopra group has examined crystal structures of diphenylselenide and diphenyltelluride,[246] which form 1D chains assembled through bifurcated Se···π and Te···π interactions, respectively. Intramolecular pnictogen bonds to π-systems have been shown to influence arsenic-based macrocycle assembly by aiding molecular preorganization during macrocycle synthesis and imparting additional stability to the macrocycles under acidic conditions.[247] Theoretical calculations suggest chalcogen/pnictogen···π interactions are robust and potentially stronger than halogen···π interactions,[248] further supporting the potential of such interactions for cocrystal design.

A prominent example of using chalcogen bonds to carbon comes from Smirnov *et al.*,[249] who reported cocrystals based on two perfluorinated diaryltellurides chalcogen-bonded to mono- or diisocyanide coformers (Fig. 15a). The cocrystals are assembled through directional chalcogen bonds to isocyanide moieties (C–Te···C angles = 156.6–170.7°), along with several instances of C–Te···π interactions. Energy decomposition analysis indicates these chalcogen bond interactions with isocyanides are dominated by electrostatic contributions, while interactions with π-systems are dominated by dispersion contributions. A current difficulty in chalcogen bonded cocrystal design is the small number of chalcogen bond donors available for study. Nevertheless, the highlighted example, along with a recent report[250] on chalcogen-bonded cocrystallisation of a perfluorinated diaryltelluride with naphthalene, phenanthrene, pyrene and triphenylene, clearly points to a very strong potential of such molecules to form chalcogen bonds not only to electron lone pairs but also to more disperse π-systems found in PAHs.

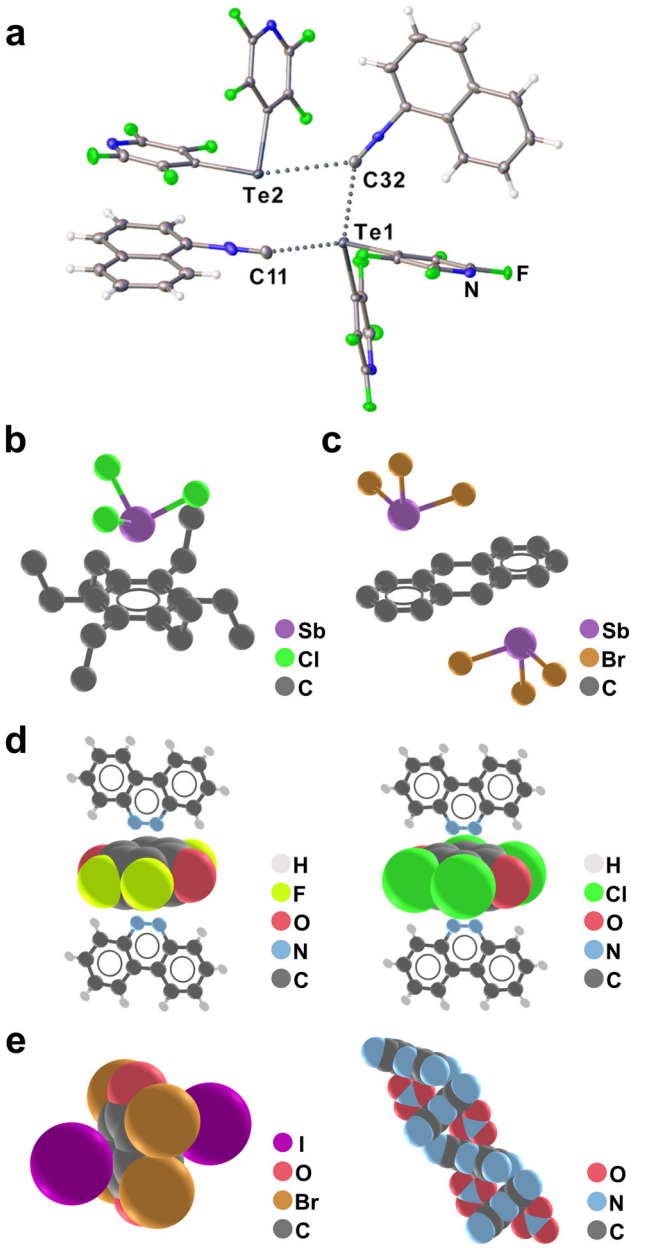

Fig. 15 (a) Fragment of the structure of the cocrystal assembled through chalcogen bonds to isocyanide moieties (adapted with permission.[249] Copyright 2024, American Chemical Society). Molecular assemblies in cocrystals of: (b) $SbCl_3$ and hexaethylbenzene;[256] (c) $SbBr_3$ and 9,10-dihydroanthracene;[257] (d) $(BC)_2$(tetrafluoro-1,4-benzoquinone) (left) and $(BC)_2$(tetrachloro-1,4-benzoquinone) (right).[268] e) Anion···π sandwich assemblies of tetrabromo-1,4-benzoquinone and iodide anions (left),[274] and chain motif of tetracyanopyrazine and nitro anions (right).[276]

Menshutkin complexes

The ability of heavy-pnictogen halides to form solid-state complexes with arenes has been explored since the end of the 19th century,[251,252] spurred by the observation that trihalides of antimony and arsenic are often soluble in non-polar aromatic solvents.[253] Materials obtained from such solutions were found to have higher thermal stability than the individual starting components, indicative of solid-state complex formation. In depth studies of these solids by Menshutkin focused on determining the compositions of the complexes, as well as their thermal properties, earning the namesake "Menshutkin complexes".[254] From the mid-20th century, Menshutkin complexes have attracted interest from a structural perspective, as well as for understanding the role of pnictogen bonds to π-systems in reaction mechanisms.[255] Generally, pnictogen trihalides are found to crystallise with arenes in 1:1 or 2:1 stoichiometric ratios, with the pnictogen atom typically

positioned over the center, or slightly off-center, of the aromatic ring. The two stoichiometries correspond to assembly motifs in which the pnictogen bonds form to either one, or both, faces of the arene.

For example, Schmidbaur *et al.*[256] reported the crystal structure of antimony(III) chloride ($SbCl_3$) and hexaethylbenzene (C_6Et_6), with the composition $(SbCl_3)(C_6Et_6)$, in which each $SbCl_3$ unit is bound to one arene with an Sb···ring distance of 2.96 Å (Fig. 15b). A cocrystal of $SbBr_3$ and 9,10-dihydroanthracene, however, adopts the 2 : 1 stoichiometry with the central acceptor interacting with two pnictogen donor units (Fig. 15c).[257] The halides AsX_3, SbX_3, and BiX_3 (X = Cl, Br) have been found to form cocrystals with a wide variety of arenes,[258,259] including naphthalene,[260] biphenyl,[261] benzene,[262] and *p*-xylene.[263] The scope of Menshutkin complexes suggests that other organo-pnictogens could be devised towards cocrystal design with arenes.

Cocrystals based on n-π*/π-hole interactions

Whereas cocrystals based on σ-hole interactions require electron-rich π-systems as recognition sites, the direct interaction between lone pairs and electron-deficient π-systems offers a contrasting recognition motif. Such interaction is referred to by several names, including n···π*, lp···π, lp···π-hole, or any other such combination, and is essentially based on electron-rich lone pairs targeting electron-poor regions of an aromatic unit, usually associated with an empty π*-orbital.[264,265] While Mooibroek *et al.*[266] noted that n···π* interactions are not uncommon across the literature, there are few cases where such interactions have been explicitly used in crystal structure design. Several examples of cocrystals assembled through n···π* interactions have relied on the presence of *cis*-azo moieties (R–N═N–R), using benzo[*c*]cinnoline (**BC**) or 2,3-diazabicyclo[2.2.2]octene (**DBO**) as coformers. Blackstock and Kochi reported the cocrystal (**DBO**)$_2$(tetracyanoethylene),[267] where the azo moiety of DBO interacts with the central double bond of tetracyanoethylene. In this case, the n···π* interaction results in charge-transfer between the two components, evident by the generation of highly-colored species in solution and in the obtained cocrystals. More recently, Bhowal *et al.*[268] examined the impact of n···π* interactions on cocrystal luminescence, demonstrating almost complete quenching of emission in **BC**-containing cocrystals. The two reported cocrystals, (**BC**)$_2$(tetrafluoro-1,4-benzoquinone) and (**BC**)$_2$(tetrachloro-1,4-benzoquinone), feature benzoquinone molecules bounded from both sides by **BC** units (Fig. 15d), with short N···C contacts ranging from 2.87 to 3.23 Å. The same work showed that other cocrystals based on π–π stacking involving either **BC** or benzoquinone are highly luminescent, indicating that the n···π* interaction is relevant for quenching.

Cocrystal design using n···π* interactions is relevant to energetic cocrystals, which often contain electron-rich substituents on electron-deficient aromatic systems. Li *et al.*[269] conducted computational analysis of reported crystal structures of energetic molecules, such as 1,3,5-triaminotrinitrobenzene, highlighting interaction energies for the generally T-shaped n···π* interactions ranging from 6.3–20.0 kJ mol^{-1}. A crucial insight related to cocrystal design is the weakness of n···π* interactions in comparison with HBs and π···π stacking, suggesting that designing cocrystals based on n···π* interactions will be most effective when using hydrogen-free or non-planar molecules.

Another topic of considerable interest is the use of anion···π and cation···π interactions in cocrystal design. Charged species are known to interact with electron-rich π-systems (cation···π interactions) and electron-deficient π-systems (anion···π interactions), acting reliably for forming complexes in solution and a variety of salt structures in the crystalline solid-state.[270,271] However, concrete strategies to employ such interactions for targeted cocrystallisation are still being developed.[272] As an example, the Rissanen group has shown the electron-rich cavities of resorcinarenes to be effective recognition sites for cations,[273] such as alkyl ammoniums or bulky protonated bases, yielding templated solid-state capsule formation. More recently, Molčanov *et al.* described a series of cocrystals containing *N*-methylpyridinium iodides and halogenated quinones, assembling into consistent I$^-$···quinone···I$^-$ anion···π motifs (Fig. 15e). The reliability of this motif was shown across a wide variety of iodide salts, with an estimated I$^-$···quinone interaction energy of −11 kcal mol^{-1}.[274]

Cocrystals of cyano- and nitro-decorated arenes with a variety of anions have been reported, exhibiting a range of different supramolecular motifs.[275] A series of such structures were analyzed by Han *et al.* who studied cocrystallisation between tetraalkylammonium salts containing different anions and a variety of π-acids.[276] The anions were found to consistently form linear 1-D chains of alternating anion and π-acid (Fig. 15e), interacting through n···π* interactions, with the alkylammonium cations surrounding the 1-D chain motifs.

Due to the large calculated interaction energies possible for anion–π interactions, it is likely that further investigations of such salt cocrystal systems will reveal more predictable structural motifs of value for targeted cocrystal design, and will help clarify or even design the role of counterions[271b] and arene substituents[277] in the formation of such structures.

Conclusions and outlook

Whereas carbon is not often seen as a target in the design of supramolecular materials, at least not outside the context of forming π-stacked supramolecular structures, the presented overview illustrates that there is a wide range of supramolecular motifs that can engage hydrocarbons and carbon-only molecular species. While this overview is not meant to be comprehensive, with each of the many different modes of self-assembly presented here deserving wider discussion, we hope that the outlined examples will inspire the crystal engineers and materials chemists to continue developing ways to exploit the simplest available carbon-based molecules in materials design. In that context, there is considerable, still emerging potential

for the use of directional interactions such as halogen bonds, and possibly also other types of σ-hole interactions,[248,249] in developing new, hydrocarbon-based architectures and functional materials. This potential is demonstrated both in the recognition of robust halogen-bonded motifs through which non-substituted arenes can be engaged in materials development,[114] as well as in the ability to design new, more complex crystal structures by repositioning hydrogen-bonded assemblies in a crystal by using halogen bonds to ''latent'' carbon moieties.[133,135] At the same time, halogen bond-driven cocrystallisation of PAHs has already been demonstrated capable of generating new materials, with interesting reactive, optical, and conductive properties.[94,100,128–130] We hope that this review will motivate further developments in this direction, and lead to new opportunities in materials design based on the solid-state supramolecular chemistry of carbon and C–H groups.

Author contributions

This article was prepared with joint contributions of both authors.

Conflicts of interest

There are no conflicts to declare.

Data availability

No primary research results, software or code have been included, and no new data were generated or analysed as part of this review.

Acknowledgements

We thank the support of the Leverhulme International Professorship, McGill University, University of Birmingham, Tier-1 Canada Research Chair Program and NSERC John C. Polanyi Award (JCP 562908-2022).

Notes and references

1 E. A. Meyer, R. K. Castellano and F. Diederich, *Angew. Chem., Int. Ed.*, 2003, **42**, 1210–1250.
2 K. Biradha and R. Santra, *Chem. Soc. Rev.*, 2013, **42**, 950–967.
3 L. Ma, G. C. George, III, S. P. Kelley and K. M. Hutchins, *J. Am. Chem. Soc.*, 2025, **147**, 18249–18256.
4 M. Cohen, G. Schmidt and F. Sonntag, *J. Chem. Soc.*, 1964, 2000–2013.
5 H. Inokuchi and H. Akamatu, in *Solid State Physics*, ed. F. Seitz and D. Turnbull, Academic Press, 1961, vol. 12, pp. 93–148.
6 M. Mas-Torrent and C. Rovira, *Chem. Rev.*, 2011, **111**, 4833–4856.
7 J. Gierschner, J. Shi, B. Milián-Medina, D. Roca-Sanjuán, S. Varghese and S. Park, *Adv. Opt. Mater.*, 2021, **9**, 2002251.
8 T. Siegrist, C. Kloc, J. H. Schön, B. Batlogg, R. C. Haddon, S. Berg and G. A. Thomas, *Angew. Chem., Int. Ed.*, 2001, **40**, 1732–1736.
9 J. E. Anthony, J. S. Brooks, D. L. Eaton and S. R. Parkin, *J. Am. Chem. Soc.*, 2001, **123**, 9482–9483.
10 (*a*) A. Kitaigorodsky, *Molecular crystals and molecules*, Elsevier, 2012; (*b*) A. M. Hiszpanski, A. R. Woll, B. Kim, C. Nuckolls and Y.-L. Loo, *Chem. Mater.*, 2017, **29**, 4311–4316; (*c*) K. E. Maly, *Cryst. Growth Des.*, 2011, **11**, 5628–5633; (*d*) L. R. MacGillivray, *CrystEngComm*, 2004, **6**, 77–78.
11 (*a*) J. D. Dunitz, *CrystEngComm*, 2003, **5**, 506; (*b*) S. Aitipamula, *et al.*, *Cryst. Growth Des.*, 2012, **12**, 2147–2152.
12 G. R. Desiraju, *J. Am. Chem. Soc.*, 2013, **135**, 9952–9967.
13 (*a*) A. S. Cannon and J. C. Warner, *Cryst. Growth Des.*, 2002, **2**, 255–257; (*b*) Y. Ding, Y. Zhao and Y. Liu, *Aggregate*, 2025, **5**, e626.
14 (*a*) M. K. Corpinot and D.-K. Bučar, *Cryst. Growth Des.*, 2019, **19**, 1426–1453; (*b*) C. Li and L. R. MacGillivray, *Chem. – Eur. J.*, 2025, **31**, e202500756.
15 (*a*) P. Metrangolo, H. Neukirch, T. Pilati and G. Resnati, *Acc. Chem. Res.*, 2005, **38**, 386–395; (*b*) N. Ramasubbu, R. Parthasarathy and P. Murray-Rust, *J. Am. Chem. Soc.*, 1986, **108**, 4308–4314; (*c*) A. Priimagi, G. Cavallo, P. Metrangolo and G. Resnati, *Acc. Chem. Res.*, 2013, **46**, 2686–2695; (*d*) G. Cavallo, P. Metrangolo, R. Milani, T. Pilati, A. Priimagi, G. Resnati and G. Terraneo, *Chem. Rev.*, 2016, **116**, 2478–2601; (*e*) T. K. Wijethunga, M. Đaković, J. Desper and C. B. Aakeröy, *Acta Cryst.*, 2017, **B73**, 163–167; (*f*) L. C. Gilday, S. W. Robinson, T. A. Barendt, M. J. Langton, B. R. Mullaney and P. D. Beer, *Chem. Rev.*, 2015, **115**, 7118–7195; (*g*) T. Clark, M. Hennemann, J. S. Murray and P. Politzer, *J. Mol. Model.*, 2007, **13**, 291–296.
16 G. R. Desiraju, *Angew. Chem., Int. Ed. Engl.*, 1995, **34**, 2311–2327.
17 K. M. Hutchins, *R. Soc. Open Sci.*, 2018, **5**, 180564.
18 (*a*) D.-K. Bučar, *Angew. Chem., Int. Ed.*, 2025, e16614; (*b*) M. C. Etter, J. C. MacDonald and J. Bernstein, *Acta Cryst.*, 1990, **B46**, 256–262.
19 Z. Zhang, H. Huang, X. Yang and L. Zang, *J. Phys. Chem. Lett.*, 2011, **2**, 2897–2905.
20 S. T. Emmerling, R. Schuldt, S. Bette, L. Yao, R. E. Dinnebier, J. Kästner and B. V. Lotsch, *J. Am. Chem. Soc.*, 2021, **143**, 15711–15722.
21 T. Rogge, N. Kaplaneris, N. Chatani, J. Kim, S. Chang, B. Punji, L. L. Schafer, D. G. Musaev, J. Wencel-Delord, C. A. Roberts, R. Sarpong, Z. E. Wilson, M. A. Brimble, M. J. Johansson and L. Ackermann, *Nat. Rev. Methods Primers*, 2021, **1**, 43.
22 C. Kang, Z. Zhang, V. Wee, A. K. Usadi, D. C. Calabro, L. S. Baugh, S. Wang, Y. Wang and D. Zhao, *J. Am. Chem. Soc.*, 2020, **142**, 12995–13002.
23 B. Lukose, A. Kuc and T. Heine, *Chem. – Eur. J.*, 2011, **17**, 2388–2392.
24 V. R. Cooper, T. Thonhauser, A. Puzder, E. Schröder, B. I. Lundqvist and D. C. Langreth, *J. Am. Chem. Soc.*, 2008, **130**, 1304–1308.
25 G. B. McGaughey, M. Gagné and A. K. Rappé, *J. Biol. Chem.*, 1998, **273**, 15458–15463.
26 K. Molčanov, V. Milašinović and B. Kojić-Prodić, *Cryst. Growth Des.*, 2019, **19**, 5967–5980.
27 R. Thakuria, N. K. Nath and B. K. Saha, *Cryst. Growth Des.*, 2019, **19**, 523–528.
28 F. J. M. Hoeben, P. Jonkheijm, E. W. Meijer and A. P. H. J. Schenning, *Chem. Rev.*, 2005, **105**, 1491–1546.
29 C. G. Claessens and J. F. Stoddart, *J. Phys. Org. Chem.*, 1997, **10**, 254–272.
30 J. K. Klosterman, Y. Yamauchi and M. Fujita, *Chem. Soc. Rev.*, 2009, **38**, 1714–1725.
31 (*a*) S. E. Wheeler and J. W. G. Bloom, *J. Phys. Chem. A*, 2014, **118**, 6133–6147; (*b*) R. G. Huber, M. A. Margreiter, J. E. Fuchs, S. von Grafenstein, C. S. Tautermann, K. R. Liedl and T. Fox, *J. Chem. Inf. Model.*, 2014, **54**, 1371–1379.
32 (*a*) S. E. Wheeler, *Acc. Chem. Res.*, 2013, **46**, 1029–1038; (*b*) S. E. Wheeler, *J. Am. Chem. Soc.*, 2025, **147**, 19738–19750; (*c*) K. Carter-Fenk and J. M. Herbert, *Chem. Sci.*, 2020, **11**, 6758–6765; (*d*) B. Schramm, M. Gray and J. M. Herbert, *J. Am. Chem. Soc.*, 2025, **147**, 3243–3260; (*e*) R. Thakuria, N. K. Nath and B. K. Saha, *Cryst. Growth Des.*, 2019, **19**, 523–528; (*f*) R. Zhao and R.-Q. Zhang, *Phys. Chem. Chem. Phys.*, 2016, **18**, 25452–25457.
33 C. R. Martinez and B. L. Iverson, *Chem. Sci.*, 2012, **3**, 2191–2201.
34 (*a*) C. A. Hunter and J. K. M. Sanders, *J. Am. Chem. Soc.*, 1990, **112**, 5525–5534; (*b*) J. H. Williams, *Acc. Chem. Res.*, 1993, **26**, 593–598; (*c*) C. Janiak, *J. Chem. Soc., Dalton Trans.*, 2000, 3885–3896.
35 (*a*) V. Colombo, L. L. Presti and A. Gavezzotti, *CrystEngComm*, 2017, **19**, 2413–2423; (*b*) A. A. Sonina, A. D. Kuimov, N. A. Shumilov, I. P. Koskin, T. Y. Kardash and M. S. Kazantsev, *Cryst. Growth Des.*, 2023, **23**, 2710–2720.

36 G. R. Desiraju and A. Gavezzotti, *Acta Cryst.*, 1989, **B45**, 473–482.
37 S. Tothadi, A. Mukherjee and G. R. Desiraju, *Chem. Commun.*, 2011, **47**, 12080–12082.
38 M. Paul and G. R. Desiraju, *Angew. Chem., Int. Ed.*, 2019, **58**, 12027–12031.
39 S. Chakraborty, L. Rajput and G. R. Desiraju, *Cryst. Growth Des.*, 2014, **14**, 2571–2577.
40 S. Grimme, *Angew. Chem., Int. Ed.*, 2008, **47**, 3430–3434.
41 M. Mahl, M. A. Niyas, K. Shoyama and F. Würthner, *Nat. Chem.*, 2022, **14**, 457–462.
42 M. Niyas, K. Shoyama and F. Würthner, *J. Am. Chem. Soc.*, 2024, **146**, 29728–29734.
43 M. A. Niyas, K. Shoyama and F. Würthner, *Angew. Chem., Int. Ed.*, 2023, **62**, e202302032.
44 (*a*) C. K. Prout and J. D. Wright, *Angew. Chem., Int. Ed. Engl.*, 1968, **7**, 659–667; (*b*) H. Jiang, P. Hu, J. Ye, K. K. Zhang, Y. Long, W. Hu and C. Kloc, *J. Mater. Chem. C*, 2018, **6**, 1884–1902.
45 (*a*) C. R. Patrick and G. S. Prosser, *Nature*, 1960, **187**, 1021; (*b*) B. J. J. Timmer and T. J. Mooibroek, *J. Chem. Ed.*, 2021, **98**, 540–545; (*c*) J. C. Bear, R. E. Ghosh and J. K. Cockcroft, *Cryst. Growth Des.*, 2024, **24**, 3021–3029.
46 T. Dahl, *Acta Chem. Scand.*, 1975, **29a**, 170–174.
47 T. Dahl, *Acta Chem. Scand.*, 1971, **25**, 1031–1039.
48 T. Dahl, *Acta Cryst.*, 1977, **B33**, 3021–3024.
49 J. C. Collings, K. P. Roscoe, R. L. Thomas, A. S. Batsanov, L. M. Stimson, J. A. K. Howard and T. B. Marder, *New J. Chem.*, 2001, **25**, 1410–1417.
50 J. C. Collings, K. P. Roscoe, E. G. Robins, A. S. Batsanov, L. M. Stimson, J. A. K. Howard, S. J. Clark and T. B. Marder, *New J. Chem.*, 2002, **26**, 1740–1746.
51 G. W. Coates, A. R. Dunn, L. M. Henling, D. A. Dougherty and R. H. Grubbs, *Angew. Chem., Int. Ed. Engl.*, 1997, **36**, 248–251.
52 G. W. Coates, A. R. Dunn, L. M. Henling, J. W. Ziller, E. B. Lobkovsky and R. H. Grubbs, *J. Am. Chem. Soc.*, 1998, **120**, 3641–3649.
53 R. Xu, V. Gramlich and H. Frauenrath, *J. Am. Chem. Soc.*, 2006, **128**, 5541–5547.
54 R. Xu, W. B. Schweizer and H. Frauenrath, *J. Am. Chem. Soc.*, 2008, **130**, 11437–11445.
55 Y. Sonoda, M. Goto, S. Tsuzuki, H. Akiyama and N. Tamaoki, *J. Fluorine Chem.*, 2009, **130**, 151–157.
56 R. Xu, W. B. Schweizer and H. Frauenrath, *Chem. – Eur. J.*, 2009, **15**, 9105–9116.
57 M. A. Sinnwell, R. H. Groeneman, B. J. Ingenthron, C. Li and L. R. MacGillivray, *Commun. Chem.*, 2021, **4**, 60.
58 P. Kissel, R. Erni, W. B. Schweizer, N. D. Rossel, B. T. King, T. Bauer, S. Götzinger, A. D. Schlüter and J. Sakamoto, *Nat. Chem.*, 2012, **4**, 287–291.
59 H. G. Drickamer, *Science*, 1967, **156**, 1183–1189.
60 L. Ciabini, M. Santoro, F. A. Gorelli, R. Bini, V. Schettino and S. Raugei, *Nat. Mater.*, 2007, **6**, 39–43.
61 Y. Wang, L. Wang, H. Zheng, K. Li, M. Andrzejewski, T. Hattori, A. Sano-Furukawa, A. Katrusiak, Y. Meng, F. Liao, F. Hong and H.-K. Mao, *J. Phys. Chem. C*, 2016, **120**, 29510–29519.
62 Y. Wang, X. Dong, X. Tang, H. Zheng, K. Li, X. Lin, L. Fang, G. A. Sun, X. Chen, L. Xie, C. L. Bull, N. P. Funnell, T. Hattori, A. Sano-Furukawa, J. Chen, D. K. Hensley, G. D. Cody, Y. Ren, H. H. Lee and H.-K. Mao, *Angew. Chem., Int. Ed.*, 2019, **58**, 1468–1473.
63 A. Friedrich, I. E. Collings, K. F. Dziubek, S. Fanetti, K. Radacki, J. Ruiz-Fuertes, J. Pellicer-Porres, M. Hanfland, D. Sieh, R. Bini, S. J. Clark and T. B. Marder, *J. Am. Chem. Soc.*, 2020, **142**, 18907–18923.
64 M. D. Ward, W. S. Tang, L. Zhu, D. Popov, G. D. Cody and T. A. Strobel, *Macromolecules*, 2019, **52**, 7557–7563.
65 J. Alfuth, J. Chojnacki, T. Połoński, A. Herman, M. J. Milewska and T. Olszewska, *Cryst. Growth Des.*, 2022, **22**, 3493–3504.
66 J. D. Dunitz and W. B. Schweizer, *Chem. – Eur. J.*, 2006, **12**, 6804–6815.
67 J. D. Dunitz and R. Taylor, *Chem. – Eur. J.*, 1997, **3**, 89–98.
68 L. Sun, W. Zhu, W. Wang, F. Yang, C. Zhang, S. Wang, X. Zhang, R. Li, H. Dong and W. Hu, *Angew. Chem., Int. Ed.*, 2017, **56**, 7831–7835.
69 Y. Xiao, L. Liu, P. Xu, F. Sun, F. Li, X. Liu, Y. Yin, J. Leng, F. Zhang and S. Jin, *Adv. Opt. Mater.*, 2024, **12**, 2400747.
70 J. Chen, W. Zhang, W. Yang, F. Xi, H. He, M. Liang, Q. Dong, J. Hou, M. Wang, G. Yu and J. Zhou, *Nat. Commun.*, 2024, **15**, 1260.
71 J. Henderson, M. Masino, L. E. Hatcher, G. Kociok-Köhn, T. Salzillo, A. Brillante, P. R. Raithby, A. Girlando and E. Da Como, *Cryst. Growth Des.*, 2018, **18**, 2003–2009.
72 K. A. Ivshin, K. Metlushka, A. Fedonin, S. K. Latypov, V. V. Khrizanforova, Y. H. Budnikova, A. E. Vandyukov, A. G. Kiiamov, A. Laskin, S. M. Avdoshenko, M. Knupfer and O. Kataeva, *Cryst. Growth Des.*, 2023, **23**, 954–964.
73 M. J. Dewar and A. R. Lepley, *J. Am. Chem. Soc.*, 1961, **83**, 4560–4563.
74 I. Sarfo, M. Zeller and S. V. Rosokha, *Cryst. Growth Des.*, 2025, **25**, 4636–4645.
75 T. Hill, D. C. Levendis and A. Lemmerer, *Acta Cryst.*, 2018, **E74**, 113–118.
76 R. K. R. Jetti, R. Boese, P. K. Thallapally and G. R. Desiraju, *Cryst. Growth Des.*, 2003, **3**, 1033–1040.
77 P. K. Thallapally, K. Chakraborty, H. L. Carrell, S. Kotha and G. R. Desiraju, *Tetrahedron*, 2000, **56**, 6721–6728.
78 (*a*) P. K. Thallapally, A. K. Katz, H. L. Carrell and G. R. Desiraju, *CrystEngComm*, 2003, **5**, 87–92; (*b*) G. R. Desiraju, *Chem. Commun.*, 2005, 2995–3001; (*c*) D. J. Sutor, *Nature*, 1992, **195**, 68–69.
79 J. Zyss, I. Ledoux-Rak, H.-C. Weiss, D. Bläser, R. Boese, P. K. Thallapally, V. R. Thalladi and G. R. Desiraju, *Chem. Mater.*, 2003, **15**, 3063–3073.
80 H. Gao, H. He, L. Zhang, Z. Feng, X. Chen and Y. Lei, *Adv. Opt. Mater.*, 2024, **12**, 2400619.
81 Y. Beldjoudi, A. Narayanan, I. Roy, T. J. Pearson, M. M. Cetin, M. T. Nguyen, M. D. Krzyaniak, F. M. Alsubaie, M. R. Wasielewski, S. I. Stupp and J. F. Stoddart, *J. Am. Chem. Soc.*, 2019, **141**, 17783–17795.
82 G. C. Mantel, K. T. Kairys, M. L. Williams, M. D. Krzyaniak, R. M. Young, R. Tempelaar and M. R. Wasielewski, *J. Am. Chem. Soc.*, 2025, **147**, 29592–29601.
83 S. Soldner, M.-J. Sun, O. Anhalt, M. B. Sárosi, M. Stolte and F. Würthner, *Adv. Funct. Mater.*, 2025, **35**, 2412843.
84 J.-J. Liu, T. Liu, S.-B. Xia, C.-X. He, F.-X. Cheng, M.-J. Lin and C.-C. Huang, *Dyes Pigm.*, 2018, **149**, 59–64.
85 A. A. Kongasseri, S. N. Ansari, S. Garain, S. M. Wagalgave and S. J. George, *Chem. Sci.*, 2023, **14**, 12548–12553.
86 P. Yu, Y. Li, H. Zhao, L. Zhu, Y. Wang, W. Xu, Y. Zhen, X. Wang, H. Dong, D. Zhu and W. Hu, *Small*, 2021, **17**, 2006574.
87 Y. Wang, H. Wu and J. F. Stoddart, *Acc. Chem. Res.*, 2021, **54**, 2027–2039.
88 Y. Wang, H. Wu, P. Li, S. Chen, L. O. Jones, M. A. Mosquera, L. Zhang, K. Cai, H. Chen, X.-Y. Chen, C. L. Stern, M. R. Wasielewski, M. A. Ratner, G. C. Schatz and J. F. Stoddart, *Nat. Commun.*, 2020, **11**, 4633.
89 Y. Wang, H. Wu, L. O. Jones, M. A. Mosquera, C. L. Stern, G. C. Schatz and J. F. Stoddart, *J. Am. Chem. Soc.*, 2023, **145**, 1855–1865.
90 Z. Liu, G. Liu, Y. Wu, D. Cao, J. Sun, S. T. Schneebeli, M. S. Nassar, C. A. Mirkin and J. F. Stoddart, *J. Am. Chem. Soc.*, 2014, **136**, 16651–16660.
91 H. A. Benesi and J. Hildebrand, *J. Am. Chem. Soc.*, 1949, **71**, 2703–2707.
92 R. S. Mulliken, *J. Am. Chem. Soc.*, 1952, **74**, 811–824.
93 (*a*) O. Hassel and K. O. Strømme, *Acta Chem. Scand.*, 1958, **12**, 1146; (*b*) O. Hassel and C. Rømming, *Q. Rev., Chem. Soc.*, 1962, **16**, 1–18.
94 (*a*) A. V. Vasilyev, S. V. Lindeman and J. K. Kochi, *Chem. Commun.*, 2001, 909–910; (*b*) A. V. Vasilyev, S. V. Lindeman and J. K. Kochi, *New J. Chem.*, 2002, **26**, 582–592; (*c*) S. V. Rosokha and J. K. Kochi, *Struct. Bond*, 2008, **126**, 137–160.
95 O. Hassel and K. O. Strømme, *Acta Chem. Scand.*, 1959, **13**, 1781–1786.
96 B. Sütay, M. Yurtsever and E. Yurtsever, *Int. J. Quantum Chem.*, 2016, **116**, 702–709.
97 S. J. Ang, A. M. Mak, M. B. Sullivan and M. W. Wong, *Phys. Chem. Chem. Phys.*, 2018, **20**, 8685–8694.
98 (*a*) D. Y. Kim, J. M. L. Madridejos, M. Ha, J.-H. Kim, D. C. Yang, C. Baig and K. S. Kim, *Chem. Commun.*, 2017, **53**, 6140–6143; (*b*) E. M. Cabaleiro-Lago and J. Rodríguez-Otero, *Phys. Chem. Chem. Phys.*, 2020, **22**, 21988–22002.
99 (*a*) E. Munusamy, R. Sedlak and P. Hobza, *ChemPhysChem*, 2011, **12**, 3253–3261; (*b*) I. S. Youn, D. Y. Kim, W. J. Cho, J. M. L. Madridejos, H. M. Lee, M. Kolaski, J. Lee, C. Baig,

S. K. Shin, M. Filatov and K. S. Kim, *J. Phys. Chem. A*, 2016, **120**, 9305–9314.
100 H. Akamatu, H. Inokuchi and Y. Matsunaga, *Nature*, 1954, **173**, 168–169.
101 (*a*) T. Uchida and H. Akamatu, *Bull. Chem. Soc. Jpn.*, 1961, **34**, 1015–1020; (*b*) J. Kommandeur and F. R. Hall, *J. Chem. Phys.*, 1961, **34**, 129–133.
102 (*a*) D. S. Reddy, D. C. Craig and G. R. Desiraju, *J. Am. Chem. Soc.*, 1996, **118**, 4090–4093; (*b*) S. V. Rosokha, I. S. Neretin, T. Y. Rosokha, J. Hecht and J. K. Kochi, *Heteroat. Chem.*, 2006, **17**, 449–459.
103 F. J. Strieter and D. H. Templeton, *J. Chem. Phys.*, 1962, **37**, 161–164.
104 (*a*) S. A. Cooke, C. M. Evans, J. H. Holloway and A. C. Legon, *J. Chem. Soc., Faraday Trans.*, 1998, **94**, 2295–2302; (*b*) H. Sun, A. Horatscheck, V. Martos, M. Bartzetko, U. Uhrig, D. Lentz, P. Schmieder and M. Nazaré, *Angew. Chem., Int. Ed.*, 2017, **56**, 6454–6458.
105 (*a*) H. Y. Gao, Q. J. Shen, X. R. Zhao, X. Q. Yan, X. Pang and W. J. Jin, *J. Mater. Chem.*, 2012, **22**, 5336–5343; (*b*) Q. Zhu, Y. J. Gao, H. Y. Gao and W. J. Jin, *J. Photochem. Photobiol., A*, 2014, **289**, 31–38.
106 H. Y. Gao, X. R. Zhao, H. Wang, X. Pang and W. J. Jin, *Cryst. Growth Des.*, 2012, **12**, 4377–4387.
107 L. Li, Z. F. Liu, W. X. Wu and W. J. Jin, *Acta Cryst.*, 2018, **B74**, 610–617.
108 H. Wang, R. X. Hu, X. Pang, H. Y. Gao and W. J. Jin, *CrystEngComm*, 2014, **16**, 7942–7948.
109 Q. J. Shen, H. Q. Wei, W. S. Zou, H. L. Sun and W. J. Jin, *CrystEngComm*, 2012, **14**, 1010–1015.
110 H. Wang and W. J. Jin, *Acta Cryst.*, 2017, **B73**, 210–216.
111 L. Li, W. X. Wu, Z. F. Liu and W. J. Jin, *New J. Chem.*, 2018, **42**, 10633–10641.
112 Q. J. Shen, X. Pang, X. R. Zhao, H. Y. Gao, H.-L. Sun and W. J. Jin, *CrystEngComm*, 2012, **14**, 5027–5034.
113 M. Mantina, A. C. Chamberlin, R. Valero, C. J. Cramer and D. G. Truhlar, *J. Phys. Chem. A*, 2009, **113**, 5806–5812.
114 J. Vainauskas, T. H. Borchers, M. Arhangelskis, L. J. McCormick McPherson, T. S. Spilfogel, E. Hamzehpoor, F. Topić, S. J. Coles, D. F. Perepichka, C. J. Barrett and T. Friščić, *Chem. Sci.*, 2023, **14**, 13031–13041.
115 C. B. Aakeröy, A. M. Beatty and B. A. Helfrich, *J. Am. Chem. Soc.*, 2002, **124**, 14425–14432.
116 A. Amonov and S. Scheiner, *ChemPhysChem*, 2024, **25**, e202400482.
117 A. Forni, S. Pieraccini, S. Rendine, F. Gabas and M. Sironi, *ChemPhysChem*, 2012, **13**, 4224–4234.
118 H. Jain, D. Sutradhar, S. Roy and G. R. Desiraju, *Angew. Chem., Int. Ed.*, 2021, **133**, 12951–12956.
119 J. C. Bear, J. K. Cockcroft, A. Rosu-Finsen and J. H. Williams, *CrystEngComm*, 2026, **28**, 101–111.
120 (*a*) E. Bosch, E. W. Reinheimer, D. K. Unruh and R. H. Groeneman, *Acta Cryst*, 2023, **E79**, 958–961; (*b*) E. Bosch, *IUCrDATA*, 2019, **4**, x190993.
121 G. Fan and D. Yan, *Adv. Opt. Mater.*, 2016, **4**, 2139–2147.
122 (*a*) Y. V. Torubaev, K. A. Lyssenko, P. Y. Barzilovich, G. A. Saratov, M. M. Shaikh, A. Singh and P. Mathur, *CrystEngComm*, 2017, **19**, 5114–5121; (*b*) C. B. Aakeröy, M. Baldrighi, J. Desper, P. Metrangolo and G. Resnati, *Chem. – Eur. J.*, 2013, **19**, 16240–16247; (*c*) M. Baldrighi, P. Metrangolo, T. Pilati, G. Resnati and G. Terraneo, *Crystals*, 2017, **7**, 332.
123 S. d'Agostino, F. Grepioni, D. Braga and B. Ventura, *Cryst. Growth Des.*, 2015, **15**, 2039–2045.
124 K. Lisac, L. S. Germann, M. Arhangelskis, M. Etter, R. E. Dinnebier, T. Friščić and D. Cinčić, *Angew. Chem., Int. Ed.*, 2025, e202517004.
125 G. Lapadula, N. Judaš, T. Friščić and W. Jones, *Chem. – Eur. J.*, 2010, **16**, 7400–7403.
126 E. A. Katlenok, M. Haukka, O. V. Levin, A. Frontera and V. Y. Kukushkin, *Chem. – Eur. J.*, 2020, **26**, 7692–7701.
127 J. Vainauskas, F. Topić, O. S. Bushuyev, C. J. Barrett and T. Friščić, *Chem. Commun.*, 2020, **56**, 15145–15148.
128 W. Wang, Y. Zhang and W. J. Jin, *Coord. Chem. Rev.*, 2020, **404**, 213107.
129 A. Azzali, S. d'Agostino, M. Capacci, F. Spinelli, B. Ventura and F. Grepioni, *CrystEngComm*, 2022, **24**, 5748–5756.
130 A. Abe, K. Goushi, M. Mamada and C. Adachi, *Adv. Mater.*, 2024, **36**, 2211160.
131 C. B. Aakeröy and K. R. Seddon, *Chem. Soc. Rev.*, 1993, **22**, 397–407.
132 M. J. Calhorda, *Chem. Commun.*, 2000, 801–809.
133 J. Vainauskas, A. Wahrhaftig-Lewis and T. Friščić, *Angew. Chem., Int. Ed.*, 2024, **63**, e202408053.
134 L. R. MacGillivray, G. S. Papaefstathiou, T. Friščić, T. D. Hamilton, D.-K. Bučar, Q. Chu, D. B. Varshney and I. G. Georgiev, *Acc. Chem. Res.*, 2008, **41**, 280–291.
135 E. H. Feld, E. Bosch, D. K. Unruh, H. R. Krueger and R. H. Groeneman, *CrystEngComm*, 2025, **27**, 5100–5103.
136 S. Y. Oh, C. W. Nickels, F. Garcia, W. Jones and T. Friščić, *CrystEngComm*, 2012, **14**, 6110–6114.
137 (*a*) M. U. Engelhardt, F. Mier, M. O. Zimmermann and F. M. Boeckler, *J. Chem. Inf. Model.*, 2025, **65**, 13132–13144; (*b*) C. Heroven, V. Georgi, G. K. Ganotra, P. Brennan, F. Wolfreys, R. C. Wade, A. E. Fernández-Montalván, A. Chaikuad and S. Knapp, *Angew. Chem., Int. Ed.*, 2018, **57**, 7220–7224; (*c*) H. Matter, M. Nazaré, S. Güssregen, D. W. Will, H. Schreuder, A. Bauer, M. Urmann, K. Ritter, M. Wagner and V. Wehner, *Angew. Chem., Int. Ed.*, 2009, **48**, 2911–2916; (*d*) Z. Xu, Z. Yang, Y. Liu, Y. Lu, K. Chen and W. Zhu, *J. Chem. Inf. Model.*, 2014, **54**, 69–78; (*e*) I. de Vries, G. Tsiompanaki, A. Perrakis and R. P. Joosten, *Protein Sci.*, 2025, **34**, e70321.
138 Y. V. Torubaev and I. V. Skabitsky, *Cryst. Growth Des.*, 2024, **24**, 8319–8333.
139 (*a*) D. Lenoir and C. Chiappe, *Chem. – Eur. J.*, 2003, **9**, 1037–1044; (*b*) R. Bianchini, C. Chiappe, D. Lenoir, P. Lemmen, R. Herges and J. Grunenberg, *Angew. Chem., Int. Ed. Engl.*, 1997, **36**, 1284–1287; (*c*) R. Robidas and C. Y. Legault, *Angew. Chem., Int. Ed.*, 2023, **62**, e202301190.
140 A. S. Mikherdov, A. S. Novikov, V. P. Boyarskiy and V. Y. Kukushkin, *Nat. Commun.*, 2020, **11**, 2921.
141 A. S. Mikherdov, R. A. Popov, A. S. Smirnov, A. A. Eliseeva, A. S. Novikov, V. P. Boyarskiy, R. M. Gomila, A. Frontera, V. Y. Kukushkin and N. A. Bokach, *Cryst. Growth Des.*, 2022, **22**, 6079–6087.
142 A. S. Smirnov, E. A. Katlenok, A. S. Mikherdov, M. A. Kryukova, N. A. Bokach and V. Y. Kukushkin, *Int. J. Mol. Sci.*, 2023, **24**, 13324.
143 A. S. Smirnov, A. S. Mikherdov, A. V. Rozhkov, R. M. Gomila, A. Frontera, V. Y. Kukushkin and N. A. Bokach, *Chem. – Asian J.*, 2023, **18**, e202300037.
144 A. J. Arduengo III, M. Kline, J. C. Calabrese and F. Davidson, *J. Am. Chem. Soc.*, 1991, **113**, 9704–9705.
145 K. B. Ghiassi, S. Y. Chen, J. Wescott, A. L. Balch and M. M. Olmstead, *Cryst. Growth Des.*, 2015, **15**, 404–410.
146 Based on CSD Version 6.01 (November 2025), refering to non-ionic structures with more than one molecular residue, without excluding structure re-determinations and endohedral fullerenes.
147 (*a*) J. L. Atwood, L. J. Barbour and A. Jerga, *Science*, 2002, **296**, 2367–2369; (*b*) E. V. Skokan, Yu. M. Shulga and S. I. Troyanov, *Phys. Rev. B*, 2018, **98**, 214106.
148 J. L. Atwood, G. A. Koutsantonis and C. L. Raston, *Nature*, 1994, **368**, 229–231.
149 X. Chen, R. A. Boulos, A. D. Slattery, J. L. Atwood and C. L. Raston, *Chem. Commun.*, 2015, **51**, 11413–11416.
150 J. W. Steed, P. C. Junk, J. L. Atwood, M. J. Barnes, C. L. Raston and R. S. Burkhalter, *J. Am. Chem. Soc.*, 1994, **116**, 10346–10347.
151 M. Makha, C. W. Evans, A. N. Sobolev and C. L. Raston, *Cryst. Growth Des.*, 2008, **8**, 2929–2932.
152 J. L. Atwood, L. J. Barbour, C. L. Raston and I. B. N. Sudria, *Angew. Chem., Int. Ed.*, 1998, **37**, 981–983.
153 T. Kawase and H. Kurata, *Chem. Rev.*, 2006, **106**, 5250–5273.
154 A. S. Filatov, M. V. Ferguson, S. N. Spisak, B. Li, C. F. Campana and M. A. Petrukhina, *Cryst. Growth Des.*, 2014, **14**, 756–762.
155 M. Yanney, F. R. Fronczek and A. Sygula, *Angew. Chem., Int. Ed.*, 2015, **54**, 11153–11156.
156 Y. Wang, Y. Li, W. Zhu, J. Liu, X. Zhang, R. Li, Y. Zhen, H. Dong and W. Hu, *Nanoscale*, 2016, **8**, 14920–14924.
157 K. Zhang, Z.-C. Chen, Y.-F. Wu, H.-R. Tian, L. Zhang, M.-L. Zhang, S.-L. Deng, Q. Zhang, S.-Y. Xie and L.-S. Zheng, *Angew. Chem., Int. Ed.*, 2025, **64**, e202417269.
158 H. Yokoi, Y. Hiraoka, S. Hiroto, D. Sakamaki, S. Seki and H. Shinokubo, *Nat. Commun.*, 2015, **6**, 8215.

159 M. Takeda, S. Hiroto, H. Yokoi, S. Lee, D. Kim and H. Shinokubo, *J. Am. Chem. Soc.*, 2018, **140**, 6336–6342.
160 D. Pham, J. Cerón Bertran, M. M. Olmstead, M. Mascal and A. L. Balch, *Org. Lett.*, 2005, **7**, 2805–2808.
161 D. Pham, J. Ceron-Bertran, M. M. Olmstead, M. Mascal and A. L. Balch, *Cryst. Growth Des.*, 2007, **7**, 75–82.
162 P. E. Georghiou, L. N. Dawe, H.-A. Tran, J. Strübe, B. Neumann, H.-G. Stammler and D. Kuck, *J. Org. Chem.*, 2008, **73**, 9040–9047.
163 Y. Shoji, T. Kajitani, F. Ishiwari, Q. Ding, H. Sato, H. Anetai, T. Akutagawa, H. Sakurai and T. Fukushima, *Chem. Sci.*, 2017, **8**, 8405–8410.
164 A. Sygula, F. R. Fronczek, R. Sygula, P. W. Rabideau and M. M. Olmstead, *J. Am. Chem. Soc.*, 2007, **129**, 3842–3843.
165 A. Heskia, T. Maris and J. D. Wuest, *Acc. Chem. Res.*, 2020, **53**, 2472–2482.
166 M. Yamamura, T. Saito and T. Nabeshima, *J. Am. Chem. Soc.*, 2014, **136**, 14299–14306.
167 A. Heskia, T. Maris and J. D. Wuest, *Cryst. Growth Des.*, 2019, **19**, 5390–5406.
168 A. Heskia, T. Maris and J. D. Wuest, *Cryst. Growth Des.*, 2019, **19**, 5418–5428.
169 A. Heskia, T. Maris, P. M. Aguiar and J. D. Wuest, *J. Am. Chem. Soc.*, 2019, **141**, 18740–18753.
170 A. Heskia, T. Maris and J. D. Wuest, *Cryst. Growth Des.*, 2020, **20**, 1319–1327.
171 B. T. King, M. M. Olmstead, K. K. Baldridge, B. Kumar, A. L. Balch and J. A. Gharamaleki, *Chem. Commun.*, 2012, **48**, 9882–9884.
172 J. Sun, Z. Deng, D. Lee Phillips and J. Liu, *Proc. Natl. Acad. Sci. U. S. A.*, 2025, **122**, e2426059122.
173 C. Zhu, K. Shoyama, M. A. Niyas and F. Würthner, *J. Am. Chem. Soc.*, 2022, **144**, 16282–16286.
174 C. Tang, H. Han, R. Zhang, L. S. de Moraes, Y. Qi, G. Wu, C. G. Jones, I. H. Rodriguez, Y. Jiao, W. Liu, X. Li, H. Chen, L. Bancroft, X. Zhao, C. L. Stern, Q.-H. Guo, M. D. Krzyaniak, M. R. Wasielewski, H. M. Nelson, P. Li and J. F. Stoddart, *J. Am. Chem. Soc.*, 2024, **146**, 20158–20167.
175 H. He, Y. J. Lee, Z. Zong, N. Liu, V. M. Lynch, J. Kim, J. Oh, D. Kim, J. L. Sessler and X.-S. Ke, *J. Am. Chem. Soc.*, 2024, **146**, 543–551.
176 D. M. Eichhorn, S. Yang, W. Jarrell, T. F. Baumann, L. S. Beall, A. J. P. White, D. J. Williams, A. G. M. Barrett and B. M. Hoffman, *J. Chem. Soc., Chem. Commun.*, 1995, 1703–1704.
177 P. D. W. Boyd, M. C. Hodgson, C. E. F. Rickard, A. G. Oliver, L. Chaker, P. J. Brothers, R. D. Bolskar, F. S. Tham and C. A. Reed, *J. Am. Chem. Soc.*, 1999, **121**, 10487–10495.
178 S. Selmani and D. J. Schipper, *Chem. – Eur. J.*, 2019, **25**, 6673–6692.
179 E. M. Pérez and N. Martín, *Chem. Soc. Rev.*, 2008, **37**, 1512–1519.
180 M. M. Olmstead, D. A. Costa, K. Maitra, B. C. Noll, S. L. Phillips, P. M. Van Calcar and A. L. Balch, *J. Am. Chem. Soc.*, 1999, **121**, 7090–7097.
181 M. Roy, I. D. Diaz Morillo, X. B. Carroll, M. M. Olmstead and A. L. Balch, *Cryst. Growth Des.*, 2020, **20**, 5596–5609.
182 A. L. Litvinov, D. V. Konarev, A. Y. Kovalevsky, I. S. Neretin, Y. L. Slovokhotov, P. Coppens and R. N. Lyubovskaya, *CrystEngComm*, 2002, **4**, 618–622.
183 M. Schulz-Dobrick, M. Panthöfer and M. Jansen, *Eur. J. Inorg. Chem.*, 2005, 4064–4069.
184 Y. Wang, N. Rinn, K. Eberheim, F. Ziese, J. Christmann, A. Jana, S. Nier, N. W. Rosemann, S. Sanna and S. Dehnen, *Nat. Commun.*, 2025, **16**, 7903.
185 Y. Inokuma, S. Yoshioka, J. Ariyoshi, T. Arai, Y. Hitora, K. Takada, S. Matsunaga, K. Rissanen and M. Fujita, *Nature*, 2013, **495**, 461–466.
186 F. Krupp, W. Frey and C. Richert, *Angew. Chem., Int. Ed.*, 2020, **59**, 15875–15879.
187 P.-H. Liu, L. Li, J. A. Webb, Y. Zhang and N. S. Goroff, *Org. Lett.*, 2004, **6**, 2081–2083.
188 M. B. J. Atkinson, S. V. S. Mariappan, D.-K. Bučar, J. Baltrusaitis, T. Friščić, N. G. Sinada and L. R. MacGillivray, *Proc. Natl. Acad. Sci. U. S. A.*, 2011, **108**, 10974–10979.
189 Y. Yamamoto, E. Tsurumaki, K. Wakamatsu and S. Toyota, *Angew. Chem., Int. Ed.*, 2018, **57**, 8199–8202.
190 T. Steiner, *Angew. Chem., Int. Ed.*, 2002, **41**, 48–76.
191 (*a*) S. Toyota, Y. Yamamoto, K. Wakamatsu, E. Tsurumaki and A. Muñoz-Castro, *Bull. Chem. Soc. Jpn.*, 2019, **92**, 1721–1728; (*b*) T. Mitani, E. Tsurumaki and S. Toyota, *Chem. – Eur. J.*, 2023, **29**, e202203462.
192 S. Pekker, É. Kováts, G. Oszlányi, G. Bényei, G. Klupp, G. Bortel, I. Jalsovszky, E. Jakab, F. Borondics, K. Kamarás, M. Bokor, G. Kriza, K. Tompa and G. Faigel, *Nat. Mater.*, 2005, **4**, 764–767.
193 M. Du, M. Yao, J. Dong, P. Ge, Q. Dong, É. Kováts, S. Pekker, S. Chen, R. Liu, B. Liu, T. Cui, B. Sundqvist and B. Liu, *Adv. Mater.*, 2018, **30**, 1706916.
194 G. Bortel, S. Pekker and É. Kováts, *Cryst. Growth Des.*, 2011, **11**, 865–874.
195 U. Geiser, S. K. Kumar, B. M. Savall, S. S. Harried, K. D. Carlson, P. R. Mobley, H. H. Wang, J. M. Williams and R. E. Botto, *Chem. Mater.*, 1992, **4**, 1077–1082.
196 Y. Zhang, J.-G. Wang, X. Sun, Q. Liu, W. Wang and Y.-B. Wang, *ChemPlusChem*, 2018, **83**, 470–477.
197 K. B. Ghiassi, F. L. Bowles, S. Y. Chen, M. M. Olmstead and A. L. Balch, *Cryst. Growth Des.*, 2014, **14**, 5131–5136.
198 (*a*) P. Izquierdo-García, J. Lión-Villar, J. M. Fernández-García and N. Martín, *Chem. Soc. Rev.*, 2025, **54**, 11089–11104; (*b*) E. M. Pérez and N. Martín, *Chem. Soc. Rev.*, 2015, **44**, 6425–6433; (*c*) Y. Xu and M. von Delius, *Angew. Chem., Int. Ed.*, 2020, **59**, 559–573; (*d*) N. Karousis, I. Suarez-Martinez, C. P. Ewels and N. Tagmatarchis, *Chem. Rev.*, 2016, **116**, 4850–4883; (*e*) D. Umadevi, S. Panigrahi and G. N. Sastry, *Acc. Chem. Res.*, 2014, **47**, 2574–2581; (*f*) V. Sgobba and D. M. Guldi, *Chem. Soc. Rev.*, 2009, **38**, 165–184.
199 A. J. Oyer, J.-M. Y. Carrillo, C. C. Hire, H. C. Schniepp, A. D. Asandei, A. V. Dobrynin and D. H. Adamson, *J. Am. Chem. Soc.*, 2012, **134**, 5018–5021.
200 T. Matsuno, M. Fujita, K. Fukunaga, S. Sato and H. Isobe, *Nat. Commun.*, 2018, **9**, 3779.
201 T. Okazaki, Y. Iizumi, S. Okubo, H. Kataura, Z. Liu, K. Suenaga, Y. Tahara, M. Yudasaka, S. Okada and S. Iijima, *Angew. Chem., Int. Ed.*, 2011, **50**, 4853–4857.
202 (*a*) D. Fong and A. Adronov, *Chem. Sci.*, 2017, **8**, 7292–7305; (*b*) P. Imin, F. Cheng and A. Adronov, *Polym. Chem.*, 2011, **2**, 411–416.
203 H. Paloniemi, T. Ääritalo, T. Laiho, H. Liuke, N. Kocharova, K. Haapakka, F. Terzi, R. Seeber and J. Lukkari, *J. Phys. Chem. B*, 2005, **109**, 8634–8642.
204 D. M. Guldi, G. M. A. Rahman, F. Zerbetto and M. Prato, *Acc. Chem. Res.*, 2005, **38**, 871–878.
205 D. M. Guldi, G. M. A. Rahman, N. Jux, N. Tagmatarchis and M. Prato, *Angew. Chem., Int. Ed.*, 2004, **43**, 5526–5530.
206 D. M. Guldi, E. Menna, M. Maggini, M. Marcaccio, D. Paolucci, F. Paolucci, S. Campidelli, M. Prato, G. M. A. Rahman and S. Schergna, *Chem. – Eur. J.*, 2006, **12**, 3975–3983.
207 (*a*) S. Tsuzuki, *Annu. Rep. Prog. Chem., Sect. C: Phys. Chem.*, 2012, **108**, 69–95; (*b*) M. Nishio, *CrystEngComm*, 2009, **11**, 1757–1788; (*c*) M. Nishio, *CrystEngComm*, 2004, **6**, 130–158.
208 A. Guijarro, J. A. Vergés, E. San-Fabián, G. Chiappe and E. Louis, *ChemPhysChem*, 2016, **17**, 3548–3557.
209 (*a*) I. Dance and M. Scudder, *CrystEngComm*, 2009, **11**, 2233–2247; (*b*) T. Steiner, *New J. Chem.*, 2000, **24**, 137–142.
210 I. Dance and M. Scudder, *Chem. Commun.*, 1995, 1039–1040.
211 (*a*) I. Dance and M. Scudder, *Chem. – Eur. J.*, 1996, **2**, 481–486; (*b*) E. D'Oria, D. Braga and J. J. Novoa, *CrystEngComm*, 2012, **14**, 792–798; (*c*) A. Duong, A. Lévesque, C. Homand, T. Maris and J. D. Wuest, *J. Org. Chem.*, 2020, **85**, 4026–4035; (*d*) T. Steiner, *Acta Cryst.*, 2000, **56**, 1033–1034; (*e*) H. D. Arman, E. R. Rafferty, C. A. Bayse and W. T. Pennington, *Cryst. Growth Des.*, 2012, **12**, 4315–4323.
212 (*a*) S. Tsuzuki, K. Honda, T. Uchimaru, M. Mikami and A. Fujii, *J. Phys. Chem. A*, 2006, **110**, 10163–10168; (*b*) S. Scheiner, *Chem. – Eur. J.*, 2025, **31**, e202404712.
213 K. Shibasaki, A. Fujii, N. Mikami and S. Tsuzuki, *J. Phys. Chem. A*, 2007, **111**, 753–758.
214 (*a*) M. Brandl, M. S. Weiss, A. Jabs, J. Sühnel and R. Hilgenfeld, *J. Mol. Biol.*, 2001, **307**, 357–377; (*b*) A. Gil, V. Branchadell, J. Bertran and A. Oliva, *J. Phys. Chem. B*, 2007, **111**, 9372–9379; (*c*) Y. Xiao and R. J. Woods, *J. Chem. Theory Comput.*, 2023, **19**, 5503–5515.
215 C. Eger and D. A. Norton, *Nature*, 1965, **208**, 997–999.
216 P. M. Bhatt and G. R. Desiraju, *CrystEngComm*, 2008, **10**, 1747–1749.

217 P. Kádárné, *Magy. Kem. Foly.*, 1964, **70**, 325–327.
218 T. Friščić, R. W. Lancaster, L. Fábián and P. G. Karamertzanis, *Proc. Natl. Acad. Sci. U. S. A.*, 2010, **107**, 13216–13221.
219 K. J. Ardila-Fierro, V. André, D. Tan, M. T. Duarte, R. W. Lancaster, P. G. Karamertzanis and T. Friščić, *Cryst. Growth Des.*, 2015, **15**, 1492–1501.
220 Z. Luo, T. Friščić and R. Z. Khaliullin, *Phys. Chem. Chem. Phys.*, 2018, **20**, 898–904.
221 F. Topić and T. Friščić, *Can. J. Chem.*, 2020, **98**, 386–393.
222 J. H. Arevalo, E. A. Stura, M. J. Taussig and I. A. Wilson, *J. Mol. Biol.*, 1993, **231**, 103–118.
223 L. Wang, A. Hao and P. Xing, *ACS Appl. Mater. Interfaces*, 2022, **14**, 44902–44908.
224 H. Zeng, J. Xiong, Z. Zhao, J. Qiao, D. Xu, M. Miao, L. He and X. Wu, *Molecules*, 2019, **24**, 3936.
225 R. Boese, T. Clark and A. Gavezzotti, *Helv. Chim. Acta*, 2003, **86**, 1085–1100.
226 M. D. Ward, H.-T. Huang, L. Zhu, A. Biswas, D. Popov, J. V. Badding and T. A. Strobel, *Phys. Chem. Chem. Phys.*, 2018, **20**, 7282–7294.
227 K. Aoki, Y. Kakudate, M. Yoshida, S. Usuba, K. Tanaka and S. Fujiwara, *Synth. Met.*, 1989, **28**, D91–D98.
228 M. L. Cable, T. Runčevski, H. E. Maynard-Casely, T. H. Vu and R. Hodyss, *Acc. Chem. Res.*, 2021, **54**, 3050–3059.
229 T. A. Francis, H. E. Maynard-Casely, M. L. Cable, R. Hodyss and C. Ennis, *J. Phys. Chem. A*, 2023, **127**, 2322–2335.
230 E. Czaplinski, X. Yu, K. Dzurilla and V. Chevrier, *Planetary Science Journal*, 2020, **1**, 76.
231 (*a*) I. Huskić and T. Friščić, *Acta Cryst.*, 2018, **B74**, 539–559; (*b*) I. Huskić and T. Friščić, *Phil. Trans. Royal Soc. A*, 2019, **377**, 20180221; (*c*) T. Echigo and M. Kimata, *Can. Mineral.*, 2010, **48**, 1329–1357.
232 H. E. Maynard-Casely, R. Hodyss, M. L. Cable, T. H. Vu and M. Rahm, *IUCrJ*, 2016, **3**, 192–199.
233 M. L. Cable, T. H. Vu, M. J. Malaska, H. E. Maynard-Casely, M. Choukroun and R. Hodyss, *ACS Earth Space Chem.*, 2019, **3**, 2808–2815.
234 M. T. Kirchner, D. Bläser and R. Boese, *Chem. – Eur. J.*, 2010, **16**, 2131–2146.
235 E. Gagnon, A. Rochefort, V. Métivaud and J. D. Wuest, *Org. Lett.*, 2010, **12**, 380–383.
236 F. Meyer-Wegner, H.-W. Lerner and M. Bolte, *Acta Cryst.*, 2010, **C66**, 182–184.
237 V. R. Pedireddi, W. Jones, A. P. Chorlton and R. Docherty, *Chem. Commun.*, 1996, 987–988.
238 R. Siddiqui, J. Rani, H. M. Titi and R. Patra, *Coord. Chem. Rev.*, 2024, **517**, 215994.
239 G. Resnati, D. L. Bryce, G. R. Desiraju, A. Frontera, I. Krossing, A. C. Legon, P. Metrangolo, F. Nicotra, K. Rissanen, S. Scheiner and G. Terraneo, *Pure Appl. Chem.*, 2024, **96**, 135–145.
240 V. Kumar, C. Rodrigue and D. L. Bryce, *Cryst. Growth Des.*, 2020, **20**, 2027–2034.
241 P. Scilabra, G. Terraneo, A. Daolio, A. Baggioli, A. Famulari, C. Leroy, D. L. Bryce and G. Resnati, *Cryst. Growth Des.*, 2020, **20**, 916–922.
242 Y. Xu, V. Kumar, M. J. Z. Bradshaw and D. L. Bryce, *Cryst. Growth Des.*, 2020, **20**, 7910–7920.
243 J. L. Beckmann, J. Krieft, Y. V. Vishnevskiy, B. Neumann, H.-G. Stammler and N. W. Mitzel, *Chem. Sci.*, 2023, **14**, 13551–13559.
244 B. Majhi, V. A. Lohar, P. Meena and D. Chopra, *Cryst. Growth Des.*, 2023, **23**, 7922–7938.
245 P. R. Varadwaj, A. Varadwaj, H. M. Marques and K. Yamashita, *CrystEngComm*, 2023, **25**, 1038–1052.
246 S. Bhandary, A. Sirohiwal, R. Kadu, S. Kumar and D. Chopra, *Cryst. Growth Des.*, 2018, **18**, 3734–3739.
247 W. J. Vickaryous, R. Herges and D. W. Johnson, *Angew. Chem., Int. Ed.*, 2004, **43**, 5831–5833.
248 (*a*) A. Bauzá, D. Quiñonero, P. M. Deyà and A. Frontera, *CrystEngComm*, 2013, **15**, 3137–3144; (*b*) S. Scheiner, *Polyhedron*, 2021, **193**, 114905.
249 A. S. Smirnov, A. V. Rozhkov, M. A. Kryukova, V. V. Suslonov, A. Y. Ivanov, R. M. Gomila, A. Frontera, V. Y. Kukushkin and N. A. Bokach, *Cryst. Growth Des.*, 2024, **24**, 10393–10402.
250 A. S. Smirnov, A. V. Rozhkov, S. Burguera, A. Frontera, Y. V. Torubaev, N. A. Bokach and V. Y. Kukushkin, *Cryst. Growth Des.*, 2026, **26**, 635–646.
251 W. Smith and G. Davis, *J. Chem. Soc., Trans.*, 1882, **41**, 411–412.
252 W. Smith, *J. Chem. Soc., Trans.*, 1879, **35**, 309–311.
253 S. Tołłoczko, *Z. Phys. Chem.*, 1899, **30U**, 705–710d.
254 H. Schmidbaur and A. Schier, *Organometallics*, 2008, **27**, 2361–2395.
255 J. Bresien, A. Schulz, M. Thomas and A. Villinger, *Eur. J. Inorg. Chem.*, 2019, 1279–1287.
256 H. Schmidbaur, R. Nowak, B. Huber and G. Mueller, *Organometallics*, 1987, **6**, 2266–2267.
257 H. Schmidbaur, R. Nowak, O. Steigelmann and G. Müller, *Chem. Ber.*, 1990, **123**, 19–22.
258 G. Bombieri, G. Peyronel and I. M. Vezzosi, *Inorg. Chim. Acta*, 1972, **6**, 349–354.
259 S. Scholz, A.-M. Fritzsche, T. Rüffer, H. Krautscheid, M. Korb, H. Lang and M. Mehring, *Z. Anorg. Allg. Chem.*, 2025, **651**, 20240019.
260 R. Hulme and J. T. Szymanski, *Acta Cryst.*, 1969, **B25**, 753–761.
261 A. Lipka and D. Mootz, *Z. Naturforsch. B*, 1982, **37**, 695–698.
262 D. Mootz and V. Händler, *Z. Anorg. Allg. Chem.*, 1986, **533**, 23–29.
263 R. Hulme and D. J. E. Mullen, *J. Chem. Soc., Dalton Trans.*, 1976, 802–804.
264 P. Politzer, J. S. Murray and T. Clark, *Phys. Chem. Chem. Phys.*, 2021, **23**, 16458–16468.
265 (*a*) M. Jemai, R. Barbas, M. Barceló-Oliver, H. Marouani, F. Albericio, A. Frontera and R. Prohens, *Cryst. Growth Des.*, 2025, **25**, 8503–8515; (*b*) H. Wang, W. Wang and W. J. Jin, *Chem. Rev.*, 2016, **116**, 5072–5104.
266 T. J. Mooibroek, P. Gamez and J. Reedijk, *CrystEngComm*, 2008, **10**, 1501–1515.
267 S. Blackstock and J. Kochi, *J. Am. Chem. Soc.*, 1987, **109**, 2484–2496.
268 R. Bhowal, S. Biswas, A. Thumbarathil, A. L. Koner and D. Chopra, *J. Phys. Chem. C*, 2019, **123**, 9311–9322.
269 S. Li, R. Gou and C. Zhang, *Cryst. Growth Des.*, 2022, **22**, 1991–2000.
270 (*a*) D.-X. Wang and M.-X. Wang, *Acc. Chem. Res.*, 2020, **53**, 1364–1380; (*b*) M. Giese, M. Albrecht and K. Rissanen, *Chem. Rev.*, 2015, **115**, 8867–8895.
271 (*a*) H. T. Chifotides and K. R. Dunbar, *Acc. Chem. Res.*, 2013, **46**, 894–906; (*b*) S. V. Rosokha, *ChemPlusChem*, 2023, **88**, e202300350; (*c*) A. Frontera, P. Gamez, M. Mascal, T. J. Mooibroek and J. Reedijk, *Angew. Chem., Int. Ed.*, 2011, **50**, 9564–9783.
272 (*a*) A. Bauzá, T. J. Mooibroek and A. Frontera, *CrystEngComm*, 2016, **18**, 10–23; (*b*) O. Shemchuk, F. Grepioni and D. Braga, *Cryst. Growth Des.*, 2020, **20**, 7230–7237; (*c*) O. Grounds, M. Zeller and S. V. Rosokha, *New J. Chem.*, 2018, **42**, 10572–10583.
273 (*a*) S. Busi, H. Saxell, R. Fröhlich and K. Rissanen, *CrystEngComm*, 2008, **10**, 1803–1809; (*b*) H. Mansikkamäki, M. Nissinen and K. Rissanen, *Chem. Commun.*, 2002, 1902–1903; (*c*) 1H. Mansikkamäki, M. Nissinen, C. A. Schalley and K. Rissanen, *New J. Chem.*, 2003, **27**, 88–97.
274 (*a*) K. Molčanov, G. Mali, J. Grdadolnik, J. Stare, V. Stilinović and B. Kojić-Prodić, *Cryst. Growth Des.*, 2018, **18**, 5182–5193; (*b*) V. Milašinović and K. Molčanov, *CrystEngComm*, 2021, **23**, 8209–8214.
275 J. Lu and J. K. Kochi, *Cryst. Growth Des.*, 2009, **9**, 291–296.
276 B. Han, J. Lu and J. K. Kochi, *Cryst. Growth Des.*, 2008, **8**, 1327–1334.
277 M. Giese, M. Albrecht, A. Valkonen and K. Rissanen, *Chem. Sci.*, 2015, **6**, 354–359.